

2013-07-10

# Novel Drug Discovery for Glioblastoma Multiforme Using Brain Tumour Initiating Cells

Nguyen, Stephanie

---

Nguyen, S. (2013). Novel Drug Discovery for Glioblastoma Multiforme Using Brain Tumour Initiating Cells (Master's thesis, University of Calgary, Calgary, Canada). Retrieved from <https://prism.ucalgary.ca>. doi:10.11575/PRISM/27130

<http://hdl.handle.net/11023/787>

*Downloaded from PRISM Repository, University of Calgary*

UNIVERSITY OF CALGARY

Novel Drug Discovery for Glioblastoma Multiforme Using Brain Tumour Initiating Cells

by

Stephanie A. Nguyen

A THESIS

SUBMITTED TO THE FACULTY OF GRADUATE STUDIES  
IN PARTIAL FULFILMENT OF THE REQUIREMENTS FOR THE  
DEGREE OF MASTER OF SCIENCE

DEPARTMENT OF NEUROSCIENCE

CALGARY, ALBERTA

JULY, 2013

© Stephanie A. Nguyen 2013

## Abstract

Glioblastoma (GBM) is the most common and aggressive adult primary brain tumour. Populations of cells with tumour initiating capacity, termed brain tumour initiating cells (BTICs), are thought to underlie the formation, growth and recurrence of GBM. As such, therapies that target this compartment may improve the otherwise poor prognosis of this disease. Here, we identified R333, a compound targeting the JAK/STAT3 pathway, as a potent inhibitor of BTIC tumourigenicity. *In vitro*, R333 dramatically decreased the viability and clonogenic potential of diverse BTIC lines. *In vivo*, systemic treatment with R348, the prodrug form of R333, was well tolerated and demonstrated favourable pharmacokinetic properties. R348 treatment was also found to lead to a significant increase in overall median survival in an orthotopic BTIC xenograft model. Altogether, these data strongly support further investigation of this compound and potentially represent the first step toward an effective molecularly targeted therapeutic for GBM.

## Acknowledgements

The success I have been so fortunate to achieve and share in, has in no small part been owed to many individuals. For introducing me to Dr. Sam Weiss and the world of brain tumours when I was starting out as a summer student, I would like to express my gratitude to Dr. John Kelly. For their technical expertise, as well as their reliable knowledge of the ins and outs of the lab, I am thankful to Rozina Hassam, Dorothea Livingstone and Orsolya Cseh. Much appreciation is also extended to Dr. Owen Stechishin for his invaluable assistance and mentorship during my time as a student in the lab. I would also like to thank the past and present members of the Weiss Lab for establishing a unique environment that has all at once been a place for discovery, productivity and development.

Acknowledgement should also be extended to our collaborators – Drs. Natalie Grinshtein, Ahmed Aman, David Uehling, Rima Al-awar, and David Kaplan – without whom much of this work would not have been possible. The Stem Cell Network and Alberta Cancer Foundation also need to be acknowledged for their generous funding support.

Last but foremost, I would like to express my gratitude to Drs. Sam Weiss and Artee Luchman, whose unconditional support and inspiring mentorship have deeply impacted my growth as a scientist and individual since I started as an undergraduate four years ago.

## Table of Contents

Abstract.....	ii
Acknowledgements .....	iii
Table of Contents .....	iv
List of Tables .....	v
List of Figures and Illustrations .....	v
List of Symbols, Abbreviations and Nomenclature .....	vi
<b>1. INTRODUCTION.....</b>	<b>1</b>
1.1 Glioblastoma Multiforme .....	1
1.2 Cancer Stem Cells.....	8
1.3 Targeted Therapeutics.....	14
1.4 JAK/STAT Signalling in Neoplasia .....	17
1.5 JAK/STAT3 as a Therapeutic Target for GBM.....	20
1.6 Novel JAK/STAT3 Inhibitors.....	23
<b>2. STATEMENT OF HYPOTHESIS.....</b>	<b>26</b>
<b>3. MATERIALS AND METHODS .....</b>	<b>27</b>
3.1 BTIC Culture .....	27
3.2 BTIC Viability and Clonogenicity Assays .....	28
3.3 Western Blotting.....	28
3.4 Pharmacokinetic Analyses.....	30
3.5 Assessment of STAT3 Targeting <i>In Vivo</i> .....	31
3.6 Kaplan-Meier Survival Study .....	32
3.7 Microscopy .....	32
3.8 Statistical Analyses .....	33
<b>4. RESULTS .....</b>	<b>34</b>
4.1 A collection of JAK/STAT3 inhibitors differentially control BTIC growth .....	34
4.2 ZM and R333 effectively decrease viability in a large panel of BTICs .....	37
4.3 R333 significantly decreases BTIC clonogenicity.....	40
4.4 R333 does not attenuate BTIC sensitivity to TMZ.....	40
4.5 R333 inhibits STAT3 with minimal effects on other signalling pathways.....	42
4.6 R348 is metabolized to R333 <i>in vivo</i> , which accumulates to relevant concentrations in the brain .....	47
4.7 Systemic R348-treatment reduces STAT3 activation <i>in vivo</i> .....	49
4.8 R348 provides a significant benefit to overall median survival .....	50
<b>5. DISCUSSION .....</b>	<b>55</b>
<b>6. CONCLUSION .....</b>	<b>61</b>
<b>7. REFERENCES.....</b>	<b>62</b>

## List of Tables

Table 1. Clinical and molecular characteristics of BTIC lines .....	29
---	----

## List of Figures and Illustrations

Figure 1. Imaging and histopathological features of glioblastoma.....	3
Figure 2. Genomic analysis of glioblastoma identifies alterations in key genes and core molecular pathways involved in diverse cellular processes.....	5
Figure 3. Three main models proposed to account for tumour heterogeneity .....	10
Figure 4. Brain tumour stem cells (BTSCs) can be isolated from human glioblastoma and display cardinal cancer stem cell features .....	11
Figure 5. Brain tumour initiating cell (BTIC) targeting therapies may be required to achieve durable tumour control .....	13
Figure 6. The JAK/STAT3 signalling pathway .....	18
Figure 7. High throughput screening on a panel of molecularly diverse BTIC lines identifies drugs targeting the JAK/STAT pathway.....	24
Figure 8. BTIC lines show varied sensitivity to different JAK/STAT3 inhibitors.....	36
Figure 9. Low micromolar doses of ZM39923 (ZM) and R333 significantly decrease BTIC viability .....	38
Figure 10. R333 effectively decreases BTIC clonogenicity .....	41
Figure 11. R333 does not adversely affect BTIC sensitivity to temozolomide (TMZ)....	44
Figure 12. R333 specifically inhibits STAT3 with negligible effects on other signalling pathways.....	46
Figure 13. Administration of R348 leads to the accumulation of R333 .....	48
Figure 14. Systemic R348 treatment reduces JAK/STAT3 signalling <i>in vivo</i> .....	51
Figure 15. Systemic administration of R348 slows tumour progression in BT147 orthotopic xenografts .....	54

## List of Symbols, Abbreviations and Nomenclature

<b>Symbol</b>	<b>Definition</b>
ANOVA	analysis of variance
BBB	blood-brain barrier
BMX	bone marrow X-linked
BTIC	brain tumour initiating cell
BTSC	brain tumour stem cell
C/EBP $\beta$	CCAAT/enhancer binding protein beta
CDKN2A	cyclin-dependent kinase inhibitor 2A
cDNA	complementary deoxyribonucleic acid
CSC	cancer stem cell
CML	chronic myeloid leukemia
DAB	3,3'-diaminobenzidine
DMEM	Dulbecco's Modified Eagle Medium
DMSO	dimethyl sulfoxide
DNA	deoxyribonucleic acid
EGF	epidermal growth factor
EGFR	epidermal growth factor receptor
EGFRvIII	epidermal growth factor receptor variant III
EPO	erythropoietin
FBS	fetal bovine serum
FGF	fibroblast growth factor
GABRA1	gamma-aminobutyric acid (GABA) A receptor, alpha 1
GBM	glioblastoma multiforme
G-CSF	granulocyte colony-stimulating factor
H&E	hematoxylin & eosin
HFA	human fetal astrocyte
HEPES	4-(2-hydroxyethyl)piperazine-1-ethanesulfonic acid
HRP	horseradish peroxidase
HTS	high throughput screen
IC <sub>50</sub>	half maximal inhibitory concentration
IL-6	interleukin-6
i.p.	intraperitoneal
IDH1	isocitrate dehydrogenase 1
JAK	Janus kinase
LC-MS	liquid chromatography-mass spectrometry
LIF	leukemia inhibitory factor
LOH	loss of heterozygosity
MGMT	O <sup>6</sup> -methylguanine methyltransferase
mRNA	messenger ribonucleic acid
mTOR	mammalian target of rapamycin
NEFL	neurofilament, light polypeptide
NES	nestin

NF1	neurofibromin-1
NOD SCID	non-obese diabetic severe combined immunodeficiency
NSC	neural stem cell
O <sup>6</sup> -MeG	O <sup>6</sup> -methylguanine
OICR	Ontario Institute for Cancer Research
PARP	poly (ADP-ribose) polymerase
PBS	phosphate buffered saline
PDGF	platelet derived growth factor
PDGFRA	platelet derived growth factor receptor A
PEG 300	polyethylene glycol 300
PFA	paraformaldehyde
PFS	progression-free survival
PI3K	phosphoinositide 3-kinase
PIAS3	protein inhibitor of activated STAT3
PTEN	phosphatase and tensin homolog
RIPA	radio-immunoprecipitation assay
RNA	ribonucleic acid
SDS PAGE	sodium dodecyl sulfate polyacrylamide gel electrophoresis
SFM	serum free medium
SH2	Src homology 2
siRNA	short interfering ribonucleic acid
SLC12A5	solute carrier family 12 (potassium/chloride transporter), member 5
SOCS3	suppressor of cytokine signalling 3
STAT	signal transducer and activator of transcription
SYT1	synaptotagmin-1
TCGA	The Cancer Genome Atlas
TMZ	temozolomide
TP53	tumour protein 53
TYK	tyrosine kinase
VEGF	vascular endothelial growth factor
WHO	World Health Organization



# 1. INTRODUCTION

## 1.1 Glioblastoma Multiforme

Malignant glial neoplasms are the most frequent primary brain tumours in adults and encompass a spectrum of different tumour types. Each type was previously distinguished by the World Health Organization (WHO) based on the premise that the tumour arose from the aberrant growth of a specific cell type. These tumours possess astrocytic, oligodendroglial, ependymal, or mixed morphology and are classified as grades I through IV based on histopathological features [1].

Glioblastoma Multiforme (GBM), a WHO grade IV astrocytoma, is the most common type of malignant glial neoplasm. While malignant gliomas seem to be more common in men than women, there are few identified risk factors. Ionizing radiation and some genetic conditions including Li-Fraumeni syndrome, Turcot syndrome and Neurofibromatosis are the only well established risk factors [2]. In North America, 2-4 new diagnoses of GBM per 100 000 are made annually, the incidence of which peaks among those aged 45 to 75 [1, 3]. Although the incidence of GBM is fairly low, among cancer patients it accounts for a substantial number of average years of life lost due to its aggression and the age at which the disease typically becomes manifest. Without treatment, the median survival is approximately 3.5 months [4]. With surgical, radio- and chemotherapeutic interventions, the median survival of GBM patients is only 14.5 months from diagnosis [1, 5]. However, this value is reflective of patients with good

Karnofsky performance scores aged 70 years or less and on average, survival is much worse. For many, durable tumour control is never achieved and interventions become largely palliative.

GBMs are characterized by rapid proliferation with widespread invasion of normal brain. As the highest grade of astrocytoma, GBMs possess histological features consistent with aggressive tumour behaviour. GBMs are defined by the presence of pronounced nuclear atypia with hyperchromatic and pleomorphic nuclei, dense cellularity, pseudo-pallisading necrosis, and an extensive neo-vasculature (**Figure 1**) [1]. Although GBMs may appear morphologically identical based on key histological features, there are two clinically distinct subgroups of GBM. Primary GBMs are more common, composing approximately 95% of cases, and arise *de novo* at a median age of 60 [6]. Secondary GBMs are less common, arise from the progression of a lower grade lesion and predominantly occur at a median age of 45 [7]. As discussed below, these tumours also have important genetic differences.

In the last several decades, substantial effort has been directed towards understanding the genomic alterations underlying the initiation and tumorigenicity of GBM. In 2008, a multi-centre collaborative effort resulted in the publication of a consensus genome for GBM. The Cancer Genome Atlas (TCGA) study looked at DNA copy number, gene expression and DNA methylation aberrations in a set of 185 primary GBMs at initial presentation and 21 GBMs at recurrence. Nucleotide sequence aberrations in 601 selected

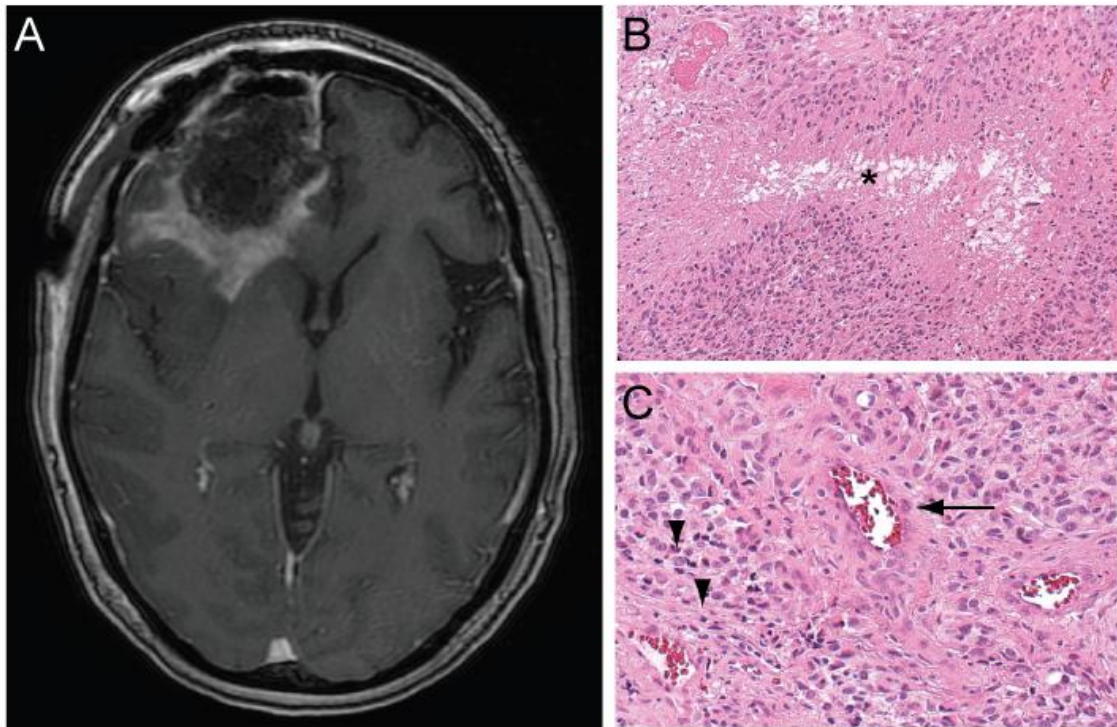


**Figure 1. Imaging and histopathological features of glioblastoma**

A, T1 weighted magnetic resonance imaging (MRI) reveals an extensive, heterogeneous mass in the right frontal lobe of a patient with recurrent glioblastoma. The severity, location and ring-like enhancement are characteristic of this tumour. B-C, Hematoxylin and eosin (H&E) staining identifies classic features of newly diagnosed GBM, including the presence of pronounced nuclear atypia, mitotically active cells (arrow heads), dense cellularity, pseudo-palisading necrosis (asterisk), and tumour vasculature (arrow).

Adapted from [8].

genes were also assessed in 91 samples in which paired normal peripheral blood or tissue was available [9]. This work has made a significant contribution to the annotation of common mutations in GBM. Not only did these results highlight and identify the frequency of previously identified molecular alterations, the integrated analyses also defined core pathways involved in GBM pathogenesis (**Figure 2**). Growth factor signalling was found to be upregulated in 88% of GBMs predominantly through mutation or amplification of the epidermal growth factor receptor (*EGFR*, 45%) and mutation or deletion of the phosphatase and tensin homolog (*PTEN*, 36%) genes, while the p53 tumour suppressor (*TP53*) pathway was altered in 87% of GBMs [9]. At the same time, Parsons *et al.* also published a study identifying genetic alterations in GBM. Unlike the TCGA, this group used an unbiased approach and sequenced 20 661 protein coding genes in 22 tumour samples. This approach resulted in the discovery of frequent mutations in the active site of the enzyme isocitrate dehydrogenase 1 (*IDH1*) [10]. *IDH1* mutation occurred in 11% of GBM patients and was found primarily in young patients and patients with secondary GBMs. Most impressively, *IDH1* mutant tumours were associated with a significantly longer overall survival compared to their wild type counterparts (3.8 vs. 1.1 years) [10].

Along side strides in the genomic profiles of GBM, large-scale transcriptomic analyses have also improved our understanding of this disease. In 2006, Phillips *et al.* identified three distinct molecular subclasses that predicted prognosis, delineated a pattern of disease progression and interestingly, resembled the stages of normal neurogenesis [11].

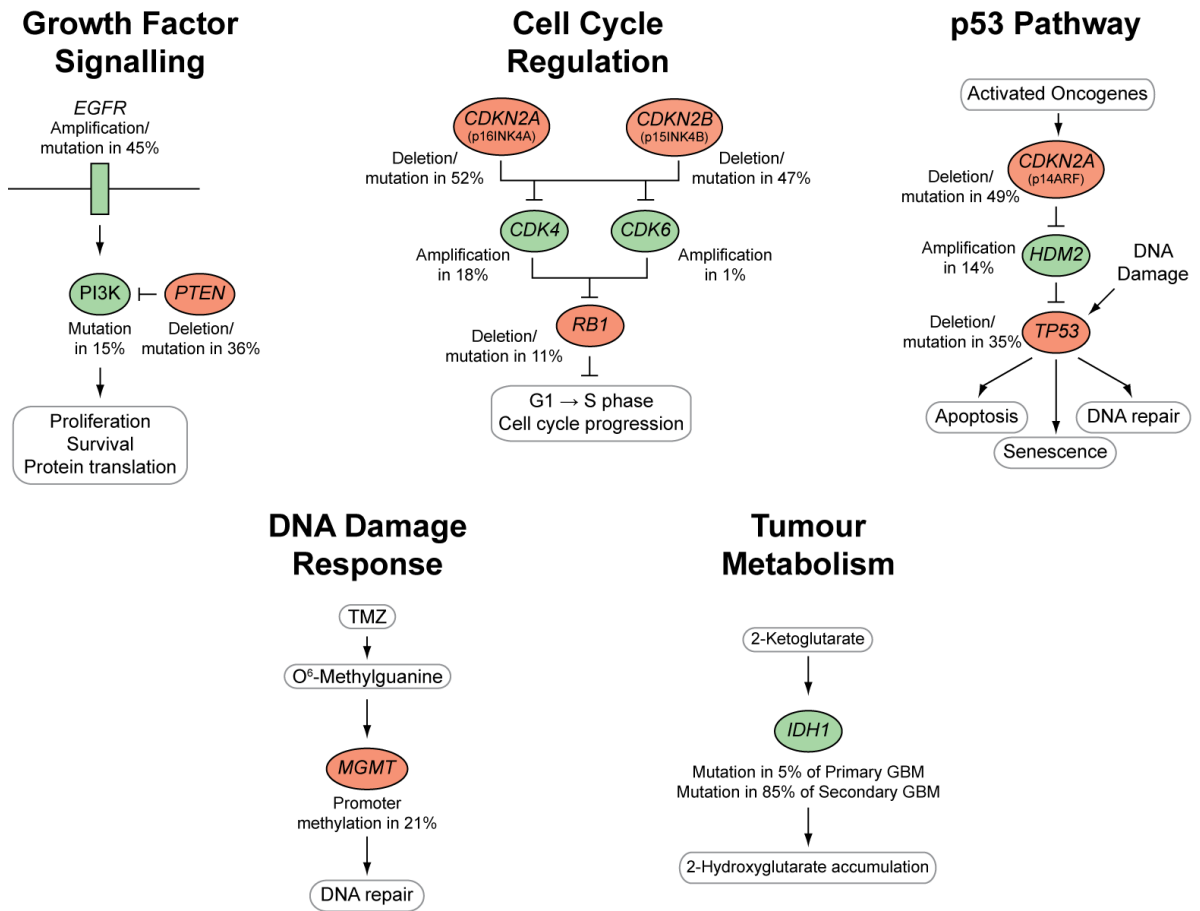


**Figure 2. Genomic analysis of glioblastoma identifies alterations in key genes and core molecular pathways involved in diverse cellular processes**

Genes with a green background are subject to amplifications or mutations that upregulate activity, whereas genes with a red background are subject to deletions or inactivating mutations. Figure adapted and modified from [9] and [10].

One class, termed by the authors as “Proneural” based on the expression of neuronal lineage markers, was found to be correlated with longer overall survival. In contrast, the other two classes, which were termed “Proliferative” and “Mesenchymal” – also for the dominant features of their respective gene signatures, were found to have similarly poor survivability.

This classification scheme was further refined in 2010, when Verhaak *et al.* integrated genomic and epigenomic data from the TCGA and other large brain tumour data sets to identify four subtypes of GBM: Classical, Mesenchymal, Proneural, and Neural [12]. The Classical subtype is characterized by chromosome 7 amplification paired with chromosome 10 loss, associated with high level *EGFR* amplification and *PTEN* loss, respectively. Additionally, although tumours of the Classical subtype show a distinct lack of *TP53* mutations, inactivation of this pathway frequently occurs through inactivation of p14ARF by focal 9p21.3 homozygous deletion targeting cyclin-dependent kinase inhibitor 2A (*CDKN2A*). The neural precursor and stem cell marker nestin (*NES*), as well as the Notch and Sonic Hedgehog signalling pathways, are also highly expressed in this subtype. Tumours of the Mesenchymal subtype often display mutations of neurofibromin-1 (*NFI*) and *PTEN* and expression of previously identified mesenchymal markers [11]. This subtype is also characterized by high expression of genes in the tumour necrosis factor super family and nuclear factor- $\kappa$ B pathways. This is thought to potentially be a consequence of higher overall necrosis and associated inflammatory infiltrates in these tumours. Furthermore, recent work has identified CCAAT/enhancer binding protein  $\beta$  (*C/EBP $\beta$* ) and signal transducer and activator of transcription 3

(STAT3) as master regulators of mesenchymal transformation. Expression of these two transcription factors induces the mesenchymal signature and was previously shown to be associated with tumour aggressiveness and poor clinical outcome [13]. Moreover, recurrent tumours often shift to a more mesenchymal signature [11]. The Proneural subtype is defined by two major features: alterations of platelet derived growth factor receptor A (*PDGFRA*) and point mutations in *IDH1*. *TP53* mutations and loss of heterozygosity (LOH) are also common in this subtype. Although this subtype is named based on the expression of several proneural genes normally expressed during development, this group of tumours also shows high expression of oligodendrocytic developmental genes. Lastly, a Neural subtype could be identified based on the expression of neuronal markers such as neurofilament, light polypeptide (*NEFL*), gamma-aminobutyric acid A receptor, alpha 1 (*GABRA1*), synaptotagmin-1(*SYT1*) and solute carrier family 12, member 5 (*SLC12A5*).

However, despite the recognition of GBM as being highly heterogeneous clinically, pathologically and at the cellular and molecular levels, as described above, the diagnosis of GBM is still based on histologic features [1]. Consequently, the four molecular subtypes of disease all remain classified as simply GBM and are treated the same in the clinic. Currently, the standard of care for GBM patients involves maximum safe resection followed by adjuvant radiation with concomitant and adjuvant temozolomide (TMZ) chemotherapy.

TMZ is an alkylating agent that functions by adding a methyl group to guanine bases in DNA, resulting in cytotoxic O<sup>6</sup>-methylguanine (O<sup>6</sup>-MeG) DNA adducts [14]. Most cells express the O<sup>6</sup>-MeG methyltransferase (MGMT) protein, which recognizes O<sup>6</sup>-MeG and cleaves off the methyl group, thereby allowing the cell to survive TMZ exposure [15]. Among GBMs, approximately 21-40% of tumours do not express MGMT protein due to methylation of the *MGMT* promoter [1, 5, 9]. Promoter methylation prevents transcription of *MGMT* mRNA and subsequent translation, thus precluding repair of O<sup>6</sup>-MeG lesions and conferring sensitivity to TMZ [5]. As a result, *MGMT* promoter methylation has become employed as a prognostic marker for GBM, and has been associated with a more favourable outcome for patients whose tumours are *MGMT* promoter methylated [15]. Despite the benefit to survival afforded with TMZ, this strategy only offers short-term tumour management. Nearly all GBMs ultimately acquire drug resistance, recur and become invariably fatal [2], such that the overall survival of GBM patients still remains only between a few months and less than five years for over 90% of patients [16].

## 1.2 Cancer Stem Cells

The initiation, growth and recurrence of many cancers have been hypothesized to be mediated by a subpopulation of tumour cells with stem-like properties, also termed cancer stem cells (CSCs) [17]. Initially, a stochastic model was proposed whereby every cell within a tumour is equivalent (**Figure 3A**). Although every cell is equivalent in this



model, the rarity of tumour initiation is attributed to the unlikelihood of any particular cell disseminated from the main tumour mass being mitotically active, while also in a permissive growth environment. This was followed by the proposition of a hierarchical model, which postulated that a population of biologically distinct cells with the capacity for self-renewal and tumour initiation reside at the apex (**Figure 3B**, reviewed in [18]). These true CSCs can produce other populations of cells that share the same tumour-initiating capacity or are more terminally differentiated. A third emerging idea is the dynamic model that maintains the CSC hierarchy but goes on to suggest that elements of the tumour microenvironment can influence more differentiated cells to change state and become more progenitor or stem-like (**Figure 3C**) [19].

The first strong evidence of the existence of CSCs was provided by experiments showing that only 1 in  $10^5$  cancer cells from a patient with acute myeloid leukemia, could recapitulate the disease when implanted into non-obese diabetic severe combined immunodeficiency (NOD SCID) mice [20]. Since then, CSCs have been identified in a multitude of cancers including GBM (reviewed in [21]). Brain tumour stem cells (BTSCs) were first identified by culturing dissociated human GBM samples using neural stem cell (NSC) techniques [22-24] (reviewed in [25]). *In vitro*, BTSCs express the NSC markers nestin and CD133 (prominin-1), self-renew and possess the potential to differentiate into neurons, astrocytes and oligodendrocytes (**Figure 4**). When implanted into the brains of neonatal rats [26] or NOD SCID mice [27], BTSCs are capable of tumour initiation and expansion as well as migration (**Figure 4**). If these cells are re-isolated from xenograft tumours, cultured *in vitro* and re-xenografted, they form

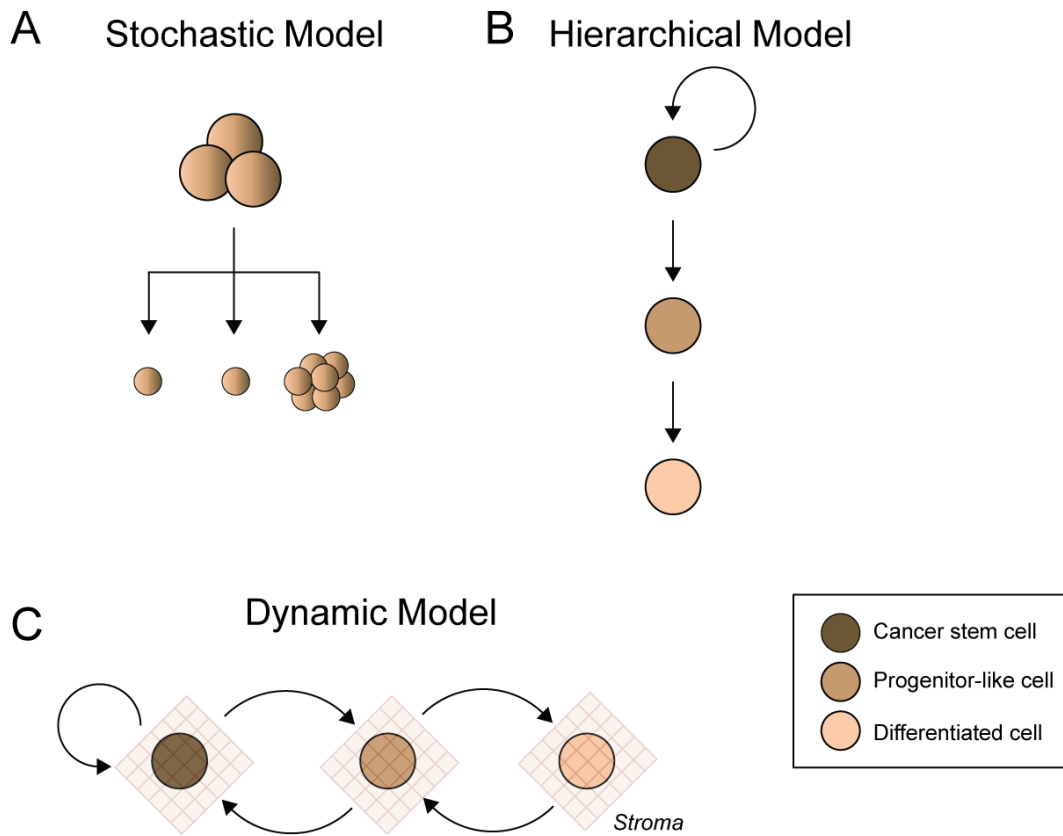


**Figure 3. Three main models proposed to account for tumour heterogeneity**

A, The stochastic model suggests that all of the cells within a tumour are equivalent but only a small proportion will initiate a tumour due to the low probability of cells being mitotically active and in an environment permissive for growth all at once. B, The hierarchical or cancer stem cell model, proposes an order in which cancer stem cells sit at the top and have the capacity to give rise to tumourigenic and non-tumourigenic/more differentiated progeny. C, The dynamic model builds on the cancer stem cell model by also suggesting that elements of the microenvironment can influence the state of a cell, by for example driving dedifferentiation. Adapted from [19].

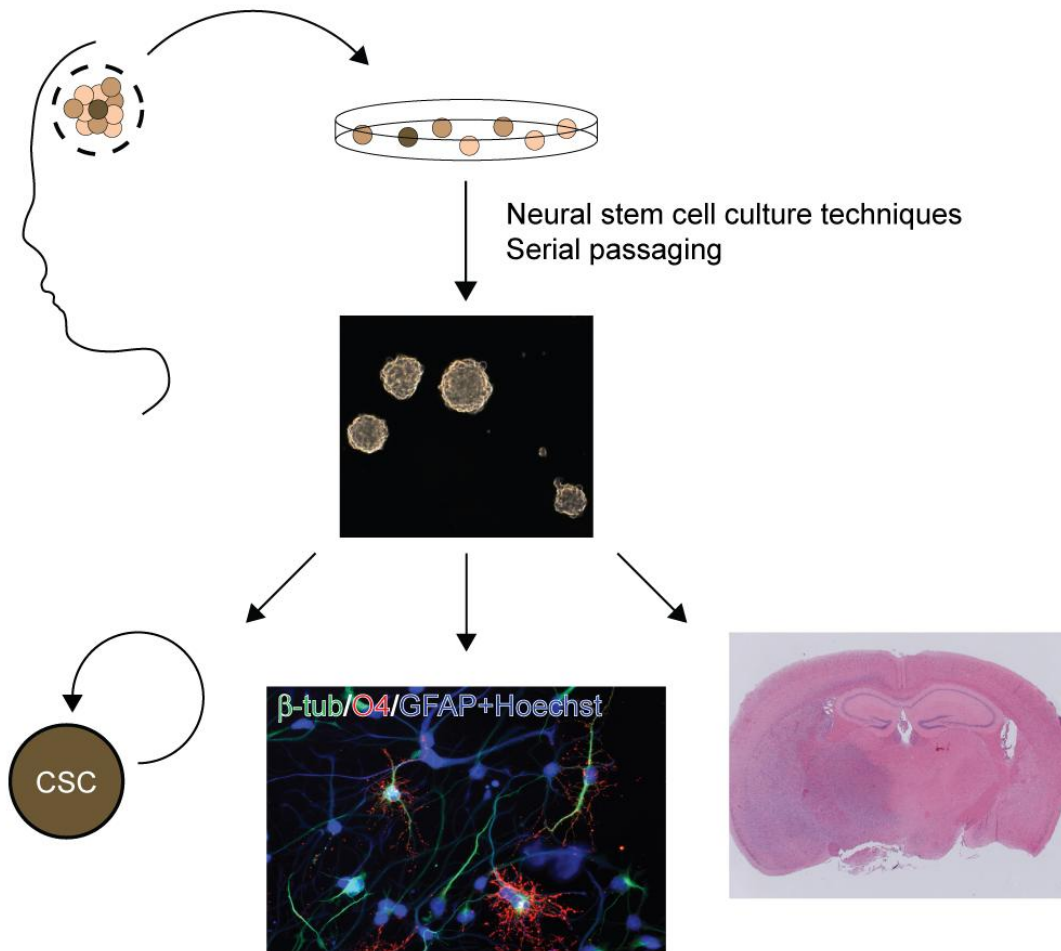


**Figure 4. Brain tumour stem cells (BTSCs) can be isolated from human glioblastoma and display cardinal cancer stem cell features**

Dissociating tissue from patient glioblastoma samples and culturing under neural stem cell conditions isolates BTSCs. Serial passages propagate BTSCs, which grow as non-adherent spheres that can be maintained in serum free medium with or without epidermal and fibroblast growth factors as stable cell lines. BTSCs demonstrate the potential to self-renew, differentiate into various neural cells ( $\beta$ -tub: neuronal marker, O4: oligodendrocyte marker, GFAP: astrocytic marker, Hoechst: nuclei stain) and initiate tumours in immune-compromised hosts. Modified from [28].

aggressive, histologically identical tumours [23], supporting their role as tumour-initiating cells [29]. This ability to readily initiate human-like tumours in mice with as few as 10 cells is perhaps the most defining property of BTSCs [28]. This has led to BTSCs being termed brain tumour initiating cells (BTICs) to better reflect this key ability, as well as sidestep the difficulty in conclusively determining differentiation state with the lack of neural lineage surface markers currently available. For the purposes of this work, the term BTIC will be used henceforth to qualify the cell lines used.

Studies have demonstrated that BTICs possess enhanced radio- and chemoresistance capabilities due to the up-regulation of pro-survival [30], drug transport [31, 32] and DNA repair pathways [33]. The extensive self-renewal and proliferative capacity of BTICs, coupled with their insensitivity to conventional therapies, suggests that BTICs may be integral to the growth and post-treatment recurrence of GBM. As such, BTICs may represent a “reservoir of disease” that will require improved understanding and novel therapeutic approaches in order to significantly improve the outcome of GBM (Figure 5).

The fact that BTICs recapitulate the genomic and transcriptomic patterns of human GBMs *in vitro* and phenocopy their parent tumours *in vivo* makes them an excellent model system for brain tumour research [29]. In the Weiss lab, we have successfully established BTIC lines from more than 80 GBM patients. Our BTIC collection includes lines isolated from treatment naïve tumours and tumours at recurrence following radio- and chemotherapy. As discussed above, recent data from the TCGA and other previous studies indicate that GBMs display frequent alterations in a core set of pathways

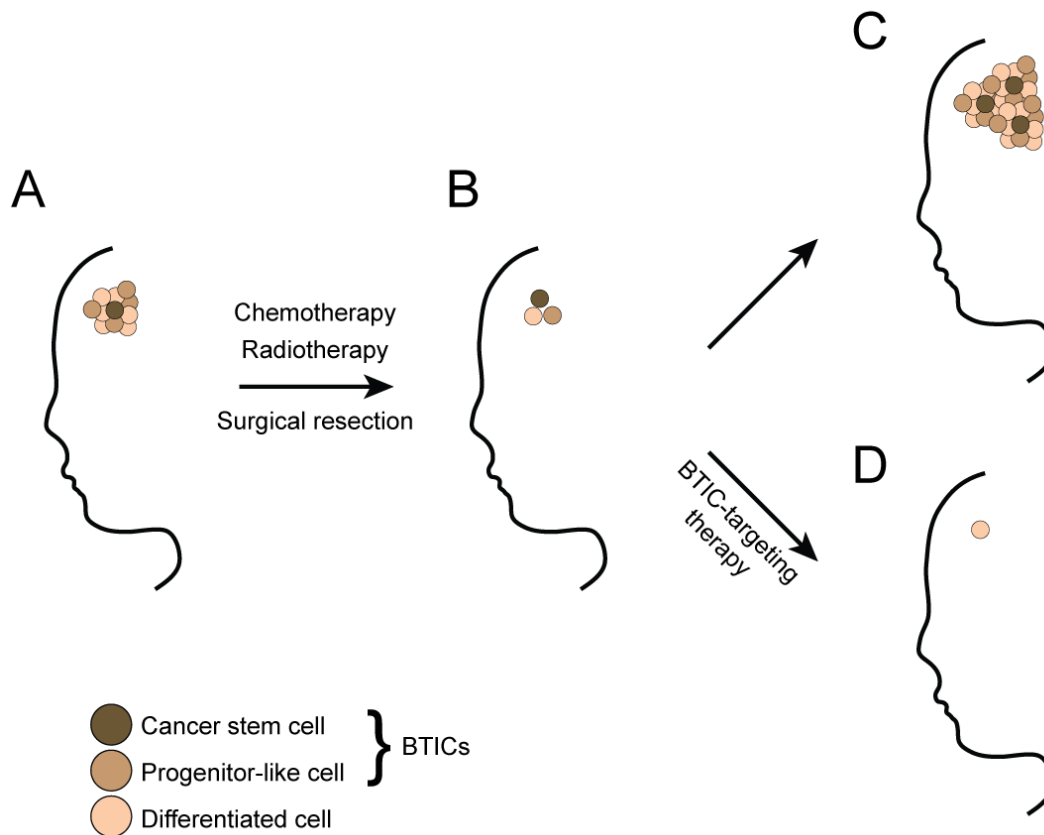


**Figure 5. Brain tumour initiating cell (BTIC) targeting therapies may be required to achieve durable tumour control**

A, Glioblastomas are composed of a heterogeneous population of various cell subtypes including those with tumour initiating capacity. B, Maximal safe surgical resection followed by standard chemo- and radiotherapy lead to tumour regression by eliminating the majority of the tumour bulk. C, Conventional therapies do not fully eliminate the compartment of cells with tumour-initiating capacity. Hence, relapse is inevitable with recurrences often becoming treatment resistant. D, The addition of BTIC-targeting therapy to the current standard of care has the potential to eliminate the tumour's ability to re-populate, resulting in long term tumour control.

regulating growth factor signalling, DNA repair, cellular senescence, and cell cycle progression. Molecular characterization has previously demonstrated that our BTIC lines retain the genetic and molecular heterogeneity of the GBMs from which they were derived [28, 34, 35]. We have successfully established several lines with endogenous mutations representative of the molecular heterogeneity of the disease [28, 35, 36]. This includes subsets with *MGMT* promoter methylation and mutations in *EGFR*, *PTEN* and *TP53* that constitute the most prevalent alterations in human GBM [9]. Taken together, this makes our BTIC collection a powerful model system for investigating GBM and evaluating novel therapeutic strategies both *in vitro* and *in vivo*.

### **1.3 Targeted Therapeutics**

The use of imatinib (Gleevec) for the treatment of chronic myeloid leukemia (CML) has become perhaps the best-known example of targeted cancer treatment. Among CML patients, over 90% possess a t(9;22) chromosomal translocation, known as the Philadelphia chromosome, that results in the BCR-ABL fusion protein. This protein functions as a constitutively active tyrosine kinase that is sufficient for oncogenic transformation [37]. Thus, it followed that imatinib, an inhibitor of ABL tyrosine kinase activity had the potential to control CML pathogenesis. In phase I and II studies, over 90% of patients showed an impressive clinical response to imatinib [38]. Subsequently, in phase III studies, imatinib more than doubled long term clinical response with fewer side effects compared to non-targeted chemotherapy. As such, imatinib became the first molecularly targeted chemotherapy regimen to be used as first-line standard of care.

Moreover, imatinib has converted CML from a progressively fatal disease to one that can be chronically controlled in the majority of patients [39].

The success of imatinib in CML has led to intense interest in identifying highly effective targeted chemotherapeutics for numerous other cancers including GBM. Advancements in our understanding of GBM at the molecular level have revealed various potential targets. One example is the vascular endothelial growth factor (VEGF) neutralizing antibody bevacizumab. GBMs are highly vascularized tumours that have been shown to express elevated levels of VEGF, an important regulator of angiogenesis [1, 40, 41]; thus, when bevacizumab was shown to produce positive results in studies of other cancers, GBM was also added to the list for evaluation. In one phase II clinical trial, eligible patients with recurrent high grade glioma received a combination of bevacizumab and irinotecan, a topoisomerase I inhibitor with which bevacizumab was previously shown to demonstrate considerable activity and safety [42, 43]. In these studies, researchers demonstrated improved radiographic response and median progression-free survival (PFS) compared to historical controls; although, the impact on overall survival was not clear [42].

Other examples from the targeted therapeutics front include clinical trials for drugs targeting EGFR. As previously mentioned, 45% of GBMs have upregulated growth factor signalling due to amplification of EGFR [9]. As such, various EGFR inhibitors have been evaluated in phase I and II clinical trials. For the most part, the outcome of these studies has been disappointing, with agents like erlotinib [44], lapatinib [45] and

gefitinib [46] demonstrating minimal activity and ultimately no improvement in overall survival or PFS. However, new strategies specifically vaccinating patients whose tumours express EGFRvIII, a frequent mutation in GBM, with a vIII-targeted peptide have been more promising. In phase II trials, PFS was prolonged to 14.2 months (vs. 6.3) and overall survival to 26 (vs. 15 months) [47].

The PI3K-PTEN-Akt-mTOR pathway has also gained renewed attention as a potential therapeutic target in the past few years. The phosphoinositide 3-kinase (PI3K) signalling pathway is altered in about 70% of GBMs, either by loss of PTEN function or amplification of various growth factor receptors – over-expression of EGFR being among the most common [9]. One of the most widely used strategies to control the aberrant signalling of this pathway has been to target mammalian target of rapamycin (mTOR), a two part complex which acts as both a downstream effector and upstream regulator of PI3K. Multiple trials have been conducted using mTOR inhibitors with outcomes ranging from partial radiographic [48] to modest histological and molecular responses [49]. However, the results of these studies have been limited and modest benefit was only achieved in subgroups of patients (reviewed in [50]).

Hence in contrast to some other cancers, targeted therapy has made only a small impact on the clinical management and outcome of GBM to date. The limited efficacy of current molecular therapies to small subsets of patients is likely in part due to the underlying heterogeneity of GBM.



## 1.4 JAK/STAT Signalling in Neoplasia

In mammals, the Janus kinase (JAK)/STAT pathway is the principal signalling mechanism for a wide array of cytokines and growth factors, enabling the rapid transduction of signals from the membrane to the nucleus. Best characterized for its role in the hematopoietic system, the pathway itself is a relatively simple sequence containing only a few principal components (reviewed in [51-53]). The JAK family is composed of four protein tyrosine kinases: JAK1/2/3 and tyrosine kinase 2 (TYK2). JAKs associate with the cytosolic domain of a variety of cytokine receptors and become activated by transphosphorylation upon cytokine binding. JAKs then recruit proteins with Src homology 2 (SH2) domains by forming docking sites on the receptor via phosphorylation of tyrosine residues. The STAT family of proteins (STAT1/2/3/5a/5b/6) are recruited to these docking sites through their SH2 domains and become phosphorylated at key tyrosine residues by JAK enzymes. This is followed by homo- or heterodimerization of STAT family members and subsequent translocation into the nucleus, where these dimers initiate the transcription of target genes. Some of these gene products drive such processes as proliferation and survival, migration and invasion, angiogenesis, and immune evasion (**Figure 6**) [54].

Much of what has been learned about JAK/STAT function has been gleaned from murine knockout studies. In TYK2 null mice, only subtle defects were observed, suggesting it was largely redundant to other JAK family members. In contrast to TYK2, JAK1 and JAK2 are key downstream mediators of multiple cytokines and growth factors. JAK1

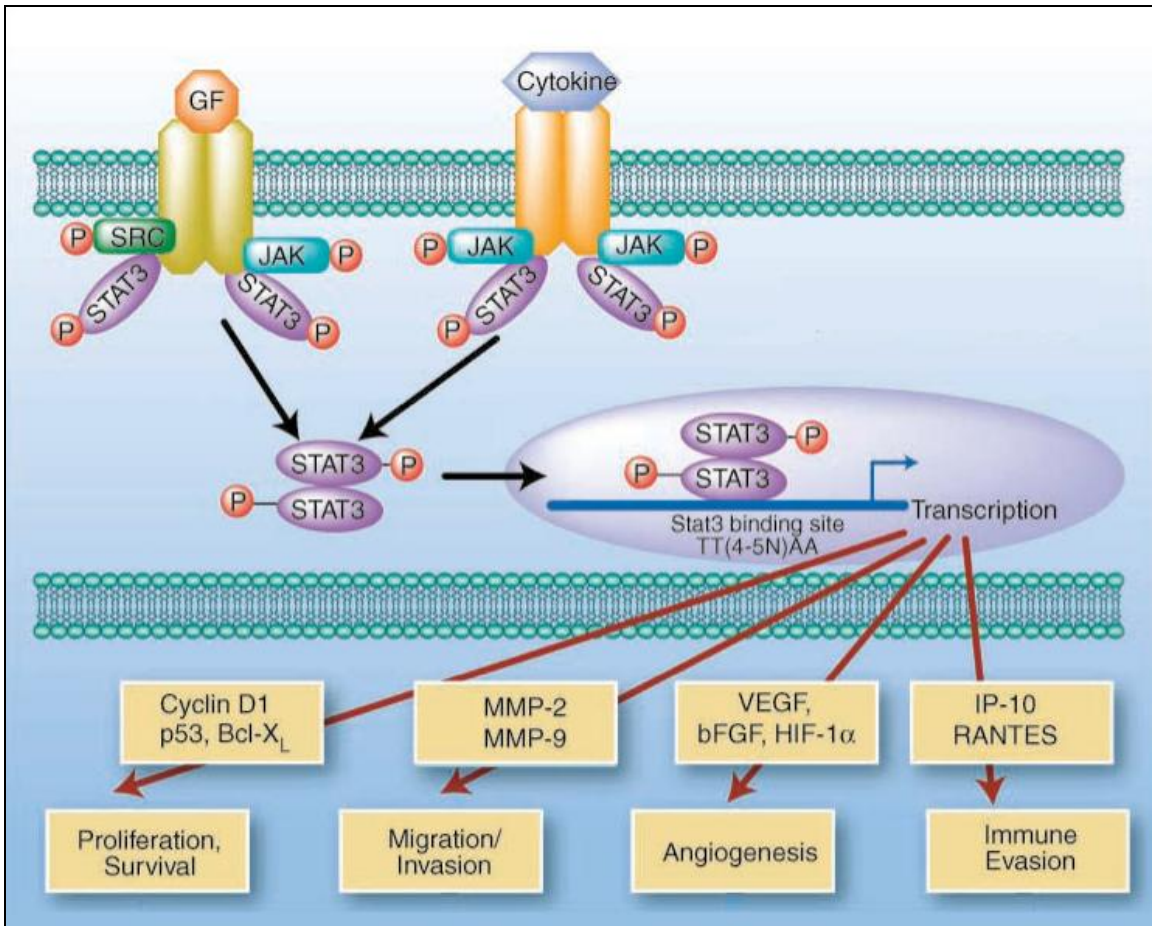


**Figure 6. The JAK/STAT3 signalling pathway**

JAKs are a family of receptor-associated cytoplasmic tyrosine kinases involved in the transduction of extracellular signals to the nucleus. Upon the binding of certain growth factors (GFs) or cytokines, pairs of JAKs become phosphorylated and in turn phosphorylate STAT3. Phosphorylated STAT3 forms dimers that translocate to the nucleus where they drive the transcription of genes controlling such processes as proliferation and survival, migration and invasion, angiogenesis, and immune evasion.

Adapted from [54].

knockouts die perinatally due to defective lymphoid development, while JAK2 knockouts die embryonically due to failed erythropoiesis. JAK3, on the other hand, has a more limited role as a downstream signalling effector and JAK3 knockouts are viable, although they display a SCID phenotype [55]. These results are not surprising given the wide expression of JAK1/2 throughout the body and the limited expression of JAK3 primarily in hematopoietic cells [56]. Among the STATs, STAT3 is unique in that it is required for development as knockouts die at embryonic day 7 with multiple severe developmental abnormalities. Conversely, knockouts of all the other STATs are completely viable. Most phenotypes consist of partial defects in the immune system, resulting in increased susceptibility to viral infections or defects in T-cell populations [57].

In addition to its roles in diverse normal cellular processes, JAK/STAT signalling can be co-opted in neoplastic transformation. Most notably, a constitutively activating V617F mutation in JAK2 is found in the majority of myeloproliferative neoplasms [58]. Mutations of the other JAKs appear to be relatively rare, but hyperactivity can be achieved by deregulation of stimulatory ligands such as erythropoietin (EPO), granulocyte colony-stimulatory factor (G-CSF), various interleukins, and growth factors including EGF and platelet derived growth factor (PDGF) [55, 57, 59]. STAT1, 3 and 5 also play a role in tumorigenesis. STAT1 is known to be pro-apoptotic and STAT1 knockouts have a significantly higher incidence of spontaneous and chemically induced tumours [60]. However, STAT3 and 5 appear to have the most consistent role in neoplasia with many diverse cancers including brain, breast, hematopoietic, head and neck, lung, kidney, prostate, and ovarian expressing activated STAT3 and/or STAT5 [61,

62]. Moreover, STAT3 is known to promote abnormal cell cycle progression, survival, angiogenesis, tissue invasion, and immune evasion. Transfection of a constitutively active form of STAT3 has been demonstrated to be sufficient to transform fibroblasts and confer tumour initiating capacity when transplanted into nude mice [63]. As such, STAT3 may be a particularly important mediator for oncogenic transformation and maintenance of a malignant phenotype.

### **1.5 JAK/STAT3 as a Therapeutic Target for GBM**

A growing body of evidence demonstrates STAT3 to be a key oncogenic signalling hub in GBM [13]. GBMs and patient-derived BTICs express high levels of activated STAT3 [13, 36]. Studies using murine and human cells have demonstrated that both STAT3 protein expression and activation by phosphorylation can be elevated through EGFR [64, 65], bone marrow X-linked (BMX) non-receptor tyrosine kinase [66], paracrine leukemia inhibitory factor (LIF) [67], interleukin-6 (IL-6) [68] and EPO [69] signalling. In addition, silencing of the STAT3 negative regulators – protein inhibitor of activated STAT3 (PIAS3) [70] and suppressor of cytokine signalling 3 (SOCS3) [71] – have been shown to mediate STAT3 activity. Furthermore, in co-operation with C/EBP $\beta$ , STAT3 has been identified as a key transcription factor for mesenchymal GBMs in a signalling network analysis [13]. Due to its role in tumourigenesis in other cancers (reviewed in [72]) and its demonstrated deregulation in GBM, STAT3 has attracted much attention as a novel potential therapeutic target.

Current strategies to block STAT3 activity focus on direct targeting of STAT3 or indirect targeting of upstream components of this pathway. Direct inhibition of STAT3 has been investigated using dominant negative STAT3 constructs [73], oligonucleotide decoys [74, 75], siRNA knockdown [76, 77], and peptidomimetics [78] that disrupt STAT3 dimerization or DNA binding. *In vitro*, these strategies have demonstrated efficacy in GBM cell lines, with effects ranging from inhibition of downstream target gene transcription to induction of apoptosis. *In vivo* validation has proven technically more difficult, but initial studies with inducible dominant negative STAT3 [73] or decoy oligonucleotides [75] have demonstrated decreased tumourigenicity and induction of apoptosis in U87 or U251 xenografts, respectively. Although these approaches have generated exciting results, limitations in their delivery and stability will likely make clinical use challenging.

Within the last few years, a number of direct pharmacological STAT3 inhibitors have been developed and tested against GBM. LLL3 and LLL12 are small molecules that inhibit STAT3 transcriptional activity by inhibiting DNA binding as well as STAT3 phosphorylation in the case of LLL12. Both compounds were found to decrease the viability of commonly used GBM cell lines, induce apoptosis and slow disease progression in xenograft models [79, 80]. Although promising, the development of agents that specifically and effectively target STAT3 activity is still in early stages. As blood-brain barrier (BBB) permeability was not demonstrated for LLL3 or LLL12, these studies were limited to intracranial drug delivery and subcutaneous xenograft models, respectively. Future agents will have to overcome this limitation in order to systemically

administer these drugs, while still achieving sufficient concentrations in the brain to be cytotoxic to tumour cells.

In contrast, the strategy to indirectly target STAT3 by disrupting upstream pathway components, like JAK, has been investigated for some time. AG490 was one of the first JAK/STAT3 inhibitors used in GBM and demonstrated efficacy in inhibiting the transcription of STAT3 target genes and inducing apoptosis [81]. AG490 was subsequently chemically modified to yield WP1066, which had increased specificity for JAK2 over JAK1 [82] and resulted in greater potency against U87 and U251 glioma cells, both *in vitro* and in subcutaneous xenografts. Two other JAK/STAT3 inhibitors derived from natural products, cucurbitacin-I [83] and curcumin [84], have also demonstrated efficacy against glioma cell lines, either as single agents or in combination with TMZ or gefitinib, an EGFR inhibitor. A new generation of small molecule JAK2 inhibitors, including AZD1480 [85] and WP1193 [86], has also been developed and demonstrate efficacy both *in vitro* and *in vivo* against human GBM cell lines and xenografts. As such, indirect inhibition of STAT3 through JAK inhibition currently represents the most readily translatable therapeutic strategy for targeting STAT3 in GBM.

In the Weiss lab, we have recently demonstrated that inhibition of JAK2 with WP1066 or cucurbitacin-I lead to on-target inhibition of downstream STAT3 signalling and dramatically reduced the survival of molecularly heterogeneous BTICs *in vitro* [36].

However, when these two drugs were tested *in vivo* using intracranial BTIC xenografts,

we were faced with the challenge of delivery and toxicity. Cucurbitacin usage was limited by systemic toxicity to animals and BBB permeability issues. WP1066 had been previously reported to effectively cross the BBB at a dose of 40 mg/kg [82] and we were able to deliver this drug systemically via intraperitoneal (i.p.) injections. This strategy demonstrated effective inhibition of JAK2/STAT3 signalling and significantly increased median survival of the treated mice. However, the drug did appear to be toxic to the mice over the time course of the treatment and the dosing had to be reduced and time course limited [36]. Altogether, these data suggest that targeting the JAK/STAT3 pathway truly is an effective means to control BTIC survival and proliferation, but highlight the need for better drugs if this is to be an amenable strategy for GBM therapy.

### **1.6 Novel JAK/STAT3 Inhibitors**

In a collaboration between Dr. Sam Weiss and Dr. David Kaplan (Hospital for Sick Children, Toronto), BTIC lines with various *EGFR*, *PTEN* and *TP53* mutational states were screened against several drug libraries. A number of promising drug targets were identified as a result of this high throughput screen (HTS), including the JAK/STAT3 pathway. The most promising inhibitor identified by the screen was ZM39923 (ZM), which almost completely eliminated the viability of 11/12 tested BTIC lines at a dose of 1  $\mu$ M. The one line that was not as completely affected was a *PTEN* and *TP53* mutant with EGFRvIII, although it was reduced to 26.7% viability at this concentration. The second most promising compound identified by the screen was Janex-1, which reduced the viability of 8/12 tested BTIC lines below 55% at 1  $\mu$ M (**Figure 7**).

		BTIC lines - 1 $\mu$ M - % viability												
		25	12	30	74	50	84	53	48	73	68	75	89	
		WT	WT	WT	WT	WT	WT	mt	mt	vIII	WT	WT	WT	EGFR status
		mt	mt	mt	mt	Het	Het	WT	Het	mt	WT	WT	WT?	PTEN status
Drug Name	Target	mt	WT	WT	WT	WT	WT	mt	WT	mt	WT	WT	WT	TP53 status
ZM39923	JAK3	0.2	0.3	0.5	3.2	0.7	0.7	1.2	0.6	26.7	1	0.7	0.4	
WHI-P 154	JAK, EGFR, Src				49	23.3	24.8	6.9			11.9	25.9	35.4	
AZ960	JAKs	19.7					51.1				40.4	14.7		
AG490	JAK2, JAK3, EGFR						24				32.1		9.4	
Janex-1	JAK3				1.4	27	47.1	0.7	48.4		40.4	42.7	50.4	

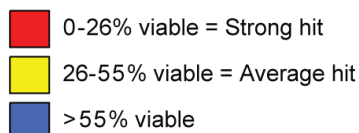


**Figure 7. High throughput screening on a panel of molecularly diverse BTIC lines identifies drugs targeting the JAK/STAT pathway**

Twelve BTICs with diverse *EGFR*, *PTEN* and *TP53* mutational status were used to screen a kinome library. Drugs were tested at 1  $\mu$ M and efficacy was determined by measuring viability. Strong hits are displayed in red, average hits in yellow and negative hits in blue. Results from the screen identified several drugs that target the JAK/STAT pathway. One of the drugs, ZM39923 was found to be highly effective on all BTIC lines, reducing viability by more than 95% in all lines except the *EGFR/PTEN/TP53* triple mutant in which it still decreased viability by approximately 75%. A second drug, Janex-1 was also modestly effective at this dose, reducing 8/12 BTIC lines to below 51% viability. WT: wildtype, mt: mutant, Het: heterozygous, vIII: variant III, ?: unknown significance. Data courtesy of N. Grinshtein and D. Kaplan.



These studies demonstrated that the majority of JAK/STAT3 targeting compounds identified in the screen had activity against JAK3. Research to date has focused on inhibiting JAK/STAT3 signalling by using inhibitors with a greater affinity for JAK2 over other JAK family members [82, 87]; however, due to its role in EPO signalling, JAK2-specific inhibitors often lead to myelosuppression that may preclude their use long term at therapeutic concentrations [88]. In contrast, JAK3 has fewer non-redundant functions in the hematopoietic and other organ systems, likely making STAT3 inhibition through a JAK3 focussed blockade more tolerable. There are a number of published JAK3 inhibitors that have not previously been tested in GBM. TCS21311 is a commercially available compound that has not yet been evaluated for any cancer [89]. Tofacitinib, also known as CP-690,550, is owned by Pfizer and has been extensively tested in phase II and III clinical trials for the treatment of various diseases including rheumatoid arthritis [90, 91], psoriasis [92, 93], dry eye [94], and ulcerative colitis [95]. Tofacitinib is also being evaluated as a means to prevent transplant rejection [96] and in early preclinical studies for adult T-cell leukemia [97]. A third example is R333, which is owned by Rigel Pharmaceuticals, and has been tested successfully in chronic animal models for cardiac allograft rejection [98], airway allograft rejection and psoriasis-like skin inflammation [99]. In the clinic, it has been tested for the treatment of Sjögren's syndrome or dry eye disease and discoid lupus erythematosus in phase I and II trials, respectively; although, the results of these studies have not yet been published.

## 2. STATEMENT OF HYPOTHESIS

GBM has a universally dim prognosis for virtually all patients. New therapies, able to achieve durable tumour control, are necessary to improve the outcome of this devastating disease. BTICs provide one of the best model systems for the preclinical development and validation of novel therapeutic strategies for GBM. Preclinical evidence from our group and others has strongly indicated that JAK/STAT3 signalling is crucial to the biology of GBM BTICs. Previous work with a number of JAK/STAT3 inhibitors has proven suboptimal during *in vivo* testing and hence unsuitable for clinical translation. However, targeting the JAK/STAT3 pathway holds tremendous promise as a therapeutic target. Therefore, we set out to use the BTIC model to identify and validate novel JAK/STAT3 inhibitors previously unexplored in GBM treatment. **We hypothesized that JAK/STAT3 inhibitors able to potently inhibit BTIC proliferation both *in vitro* and *in vivo* would be relevant as a first step towards an effective molecularly-targeted therapy for GBM patients.**

### 3. MATERIALS AND METHODS

#### 3.1 BTIC Culture

Fresh tumour samples were obtained from adult patients during their operative procedure following informed consent as previously described [28]. In brief, tumour tissue was processed by mechanical dissociation and enzymatic digestion using 200 µg/mL kynurenic acid (Sigma), 200 µg/mL collagenase (Sigma) and 500 µg/mL DNase (CalBioChem) and placed in serum-free culture medium (SFM) containing Dulbecco's Modified Eagle Medium (DMEM)/Ham's F12 (1:1) with 5 mM 4-(2-hydroxyethyl) piperazine-1-ethanesulfonic acid (HEPES) buffer, 0.6% glucose, 3 mM sodium bicarbonate, 2 mM glutamine, 25 µg/mL insulin, 100 µg/mL transferrin, 20 nM progesterone, 10 µM putrescine, and 30 nM selenite. A single cell suspension of tumour cells was obtained by further mechanical dissociation followed by filtration through a 40 µm filter. Red blood cells were removed by hypotonic lysis and tumour cells plated at 20 000 viable cells/mL. Primary cells were cultured both free of and with growth factors including: EGF (20 ng/mL, Peprotech), fibroblast growth factor-2 (FGF-2; 20 ng/mL, R&D Systems) and heparan sulfate (2 µg/mL, R&D Systems). Resulting BTIC spheres from each specimen were enzymatically dissociated (Accumax, eBioscience) and expanded to generate individual BTIC lines. Human fetal neural stem cells were also cultured as previously described [100] and induced to differentiate into astrocytes by addition of 10% fetal bovine serum (FBS) and removal of EGF, FGF- 2 and heparan sulfate. All cell lines used for this work were previously established cultures in the Weiss

lab (**Table 1**). Molecular characterization of BTIC lines was performed as previously described [35, 36].

### **3.2 BTIC Viability and Clonogenicity Assays**

BTIC spheres were chemically dissociated with Accumax (eBioscience) to single cells and seeded at 2500 cells per well in 96-well plates and treated with drug or vehicle (dimethyl sulfoxide, DMSO) 24 hours after plating. After 14-21 days, BTIC viability was assessed by performing the alamarBlue<sup>TM</sup> (Invitrogen) assay according to the manufacturer's instructions. To summarize, the assay is performed by addition of a dye that is converted by reduction in metabolically active cells to produce a fluorescent signal. This signal is measured at excitation/emission wavelengths of 540/590 nm and can in turn be used as an indicator of cell health. Drug sensitivity was also assessed using the neurosphere assay in which 100-1500 cells are seeded per well in 96-well plates, treated with drug or vehicle (DMSO) and the number of spheres counted 14-28 days later. All culture experiments were performed in triplicate with a minimum of three wells per condition.

### **3.3 Western Blotting**

BTIC spheres were chemically dissociated as above and plated at  $10^6$  cells/1.5 mL of media. Cells were treated with vehicle (DMSO) or drug and pelleted at select time points.

**Table 1. Clinical and molecular characteristics of BTIC lines**

BTIC Line	Diagnosis	Age	Sex	MGMT Methylation Status	EGFR Status	PTEN Status	TP53 Status
12	GBM-r	59	M	U	WT	FrmDel328	WT
25	GBM-r	57	M	U	WT	G129R	mt
30	GBM	67	M	U	WT	N49I	WT
42	GBM	80	M	U	A736D(?)	FrmDel298*	mt
48	GBM	68	M	Me	G598V	FrmDel17*	WT
53	GBM	59	M	Me	G598V	FrmDel329*	mt
54	OIII	49	F	Me	WT	NE	WT
63	GBM	59	F	Me	vIII	WT	WT
68	GBM	59	M	U	vIII	WT	WT
73	GBM	52	M	U	vIII	Ins intron 4	mt
75	GBM	74	M	U	WT	WT	WT
84	GBM	67	M	Me	WT	Het V341F	WT
88	OIII-r	47	M	Me	WT	Het G208V	mt
89	GBM	59	F	Me	WT	WT?	WT
90	GBM	56	M	U	vIII	Del exon 4*	WT
92	GBM-r	24	M	U	WT	R233*	mt
101	GBM	60	F	U	WT	WT	WT
108	GBM	NA	M	U	H385P	NE	mt
119	GBM-r	70	F	U	Y620C(?)	Het G36R/G165E	mt
126	GBM	67	M	Me	WT	WT	WT
143	GBM-r	46	F	Me	WT	Het G165R	mt
147	GBM-r	56	M	U	vIII	Ins T@1578*	mt

GBM: glioblastoma multiforme, OIII: anaplastic oligodendroglioma (WHO grade 3),  
-r: recurrent, Me: methylated promoter, U: unmethylated promoter, WT: wild type, mt:  
mutant, vIII: variant III, (?): unknown significance, FrmDel: frameshift deletion, Ins:  
insertion, Del: deletion, Het: heterozygous, \*: truncating alteration, NA: not available

For protein extraction, BTICs were lysed in modified radio-immunoprecipitation assay (RIPA) buffer (50 mM Tris, 150 mM NaCl, 0.1% SDS, 0.5% Na Deoxycholate, 1% NP-40) supplemented with Complete Mini protease (Roche) and Halt phosphatase (Thermo Scientific) inhibitor cocktails. Protein concentrations were quantified using the BioRad protein assay; 11-15 µg of protein were loaded on 7.5% or 12% sodium dodecyl sulfate polyacrylamide gel electrophoresis (SDS PAGE) gels and transblotted to nitrocellulose membranes. Blots were stained with primary antibodies followed by horseradish peroxidase (HRP)-conjugated secondary antibodies. Primary antibodies included p-STAT3 Y705, p-STAT3 S727, STAT3, cyclin D1, p-Akt S473, Akt, p-Erk1/2 T202/Y204, p-S6 S235/236, poly (ADP-ribose) polymerase (PARP), β-tubulin (Cell Signaling Technology), Erk1/2 (Millipore), and Actin (Santa Cruz Biotechnology). Secondary antibodies included donkey anti-mouse, donkey anti-goat (Millipore) and goat anti-rabbit (Cell Signaling Technology). Bands were visualized with the SuperSignal West Pico chemiluminescent substrate (Thermo Scientific) and Hyperfilm (Amersham).

### **3.4 Pharmacokinetic Analyses**

All pharmacokinetic analyses were performed by Dr. Ahmed Aman through a collaboration with the Ontario Institute for Cancer Research (OICR). R348 was administered via i.p. injection to mice at 25, 50 and 100 mg/kg doses. Three mice were used for each dose. At 0.5 and 5 hour time points, blood was collected and plasma separated by centrifugation. Plasma was subjected to liquid chromatography-mass spectrometry (LC-MS) to assess plasma concentrations of R348 and R333.

For brain concentration determination, R348 was administered at 50 mg/kg via i.p. injection to two mice. One mouse was sacrificed at 0.5 hours post-injection and the other at 5 hours post-injection. Brains were harvested, processed and used to analyze accumulation of R348 and R333 using LC-MS.

### **3.5 Assessment of STAT3 Targeting *In Vivo***

BTIC spheres from BT147 were enzymatically dissociated as described above, to single cell suspensions. Cells were washed in phosphate buffered saline (PBS) and re-suspended at  $10^5$  cells per 3  $\mu$ L media for orthotopic xenografts. Six NOD SCID mice were each xenografted with  $10^5$  BT147 cells stereotactically implanted into the right striatum as previously described [28]. Seven days following implants, mice were randomized into vehicle and drug cohorts and injected i.p. thrice weekly (on Monday, Wednesday and Friday) to a total of five doses. Drug-treated mice received a 50 mg/kg dose of R348 re-suspended in 100  $\mu$ L 50% polyethylene glycol 300 (PEG 300, Sigma-Aldrich) in water. Vehicle-treated mice received an equal volume of 50% PEG 300 in water. On Day 16, mice were euthanized using a lethal dose of sodium pentobarbital two hours following injection followed with transcardiac perfusion with 4% paraformaldehyde (PFA). Brains were removed, fixed in 4% PFA and cryosectioned into 12  $\mu$ m sections for assessment by histology and immunohistochemistry. Hematoxylin and eosin (H&E) staining was performed according to standard protocols. Immunohistochemistry was performed by incubating sections with primary antibodies followed by the Vectastain Elite mouse IgG

or rabbit IgG kits (Vector Laboratories) and detection with 3,3'-diaminobenzidine (DAB) substrate and hematoxylin counterstaining (Sigma-Aldrich) according to the manufacturer's instructions. Primary antibodies included anti-human nucleolin (Abcam) and p-STAT3 Y705 (Cell Signaling Technology). Secondary antibodies included biotin conjugated goat anti-mouse and goat anti-rabbit (Jackson ImmunoResearch).

### **3.6 Kaplan-Meier Survival Study**

BT147 cells were prepared and orthotopically xenografted as described in the above section into NOD SCID mice. One week post-implantation, mice were randomized into vehicle (n=6) and drug (n=8) cohorts and started on a thrice-weekly (Monday, Wednesday and Friday) treatment regimen. Drug-treated mice were injected i.p. with 40 mg/kg R348 re-suspended in 100  $\mu$ L 50% PEG 300 in water while vehicle-treated mice received an equal volume of 50% PEG 300 in water alone. The course of treatment lasted five weeks or 14 doses, after which mice were allowed to survive until significant weight loss or presentation of neurological symptoms necessitated euthanasia. Necropsy and cranial dissection were performed to confirm the presence of tumour in all animals.

### **3.7 Microscopy**

Images of BTIC cultures were captured using a Zeiss Axiovert 40 CFL inverted microscope and AxioVision software. Histology images were acquired using the



Olympus Slide Scanner and OlyVia software at the University of Calgary Regenerational Unit in Neurobiology Microscopy Facility.

### **3.8 Statistical Analyses**

Statistically significant differences between control and treated BTIC groups were evaluated by means of Student's t-test or analysis of variance (ANOVA) and Tukey's multiple comparison test. For Kaplan-Meier survival studies, statistical difference in median survival was determined by the logrank test. All analyses were performed using GraphPad Prism.

## 4. RESULTS

### 4.1 A collection of JAK/STAT3 inhibitors differentially control BTIC growth

We first asked if the identified JAK/STAT3 inhibitors could limit BTIC viability in a panel of molecularly diverse lines. For a more thorough assessment and comparison of the efficacy of the two inhibitors identified in the HTS, as well as the three similar compounds described in Section 1.6, dose response analyses using alamarBlue™ viability assays were performed. Seven BTIC lines (BTICs) with differential *EGFR/PTEN/TP53* mutational statuses were selected for preliminary comparative assessment. Human fetal astrocytes (HFAs) were used as a counterscreen control, as available, for some of the compounds.

For ZM, half maximal inhibitory concentration ( $IC_{50}$ ) values ranged between 1.01 and 2.43  $\mu\text{M}$  for the seven tested BTICs. HFAs were unaffected by ZM at all doses (**Figure 8A**). Janex-1 demonstrated  $IC_{50}$ s between 17.3 and 36.9  $\mu\text{M}$  for the BTICs and 160.7  $\mu\text{M}$  for the HFAs (**Figure 8B**). TCS21311 was variably effective at reducing BTIC viability. Tested lines showed mixed sensitivity to this compound with  $IC_{50}$  values ranging from 1.13 to 19.19  $\mu\text{M}$  (**Figure 8C**). Tofacitinib was the worst performing compound of the five tested. BTIC  $IC_{50}$  values were above 170  $\mu\text{M}$  for all but one line. The relative resistance to this compound was also shared by the HFAs (**Figure 8D**). Last, R333 demonstrated  $IC_{50}$  values ranging between 0.28 and 2.05  $\mu\text{M}$  in the BTICs and at least four times these doses in the HFAs (**Figure 8E**).

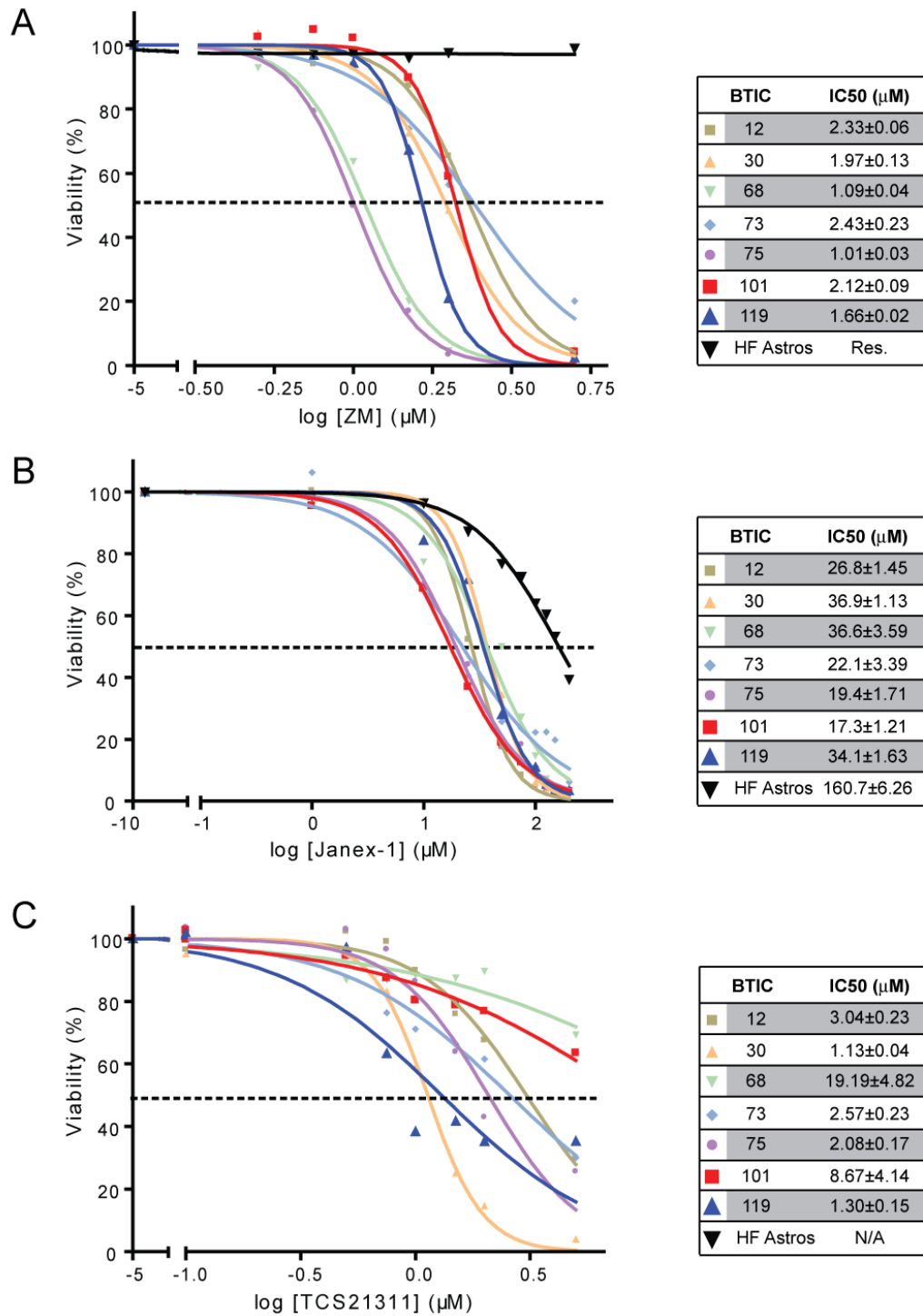


(Figure continued on next page)

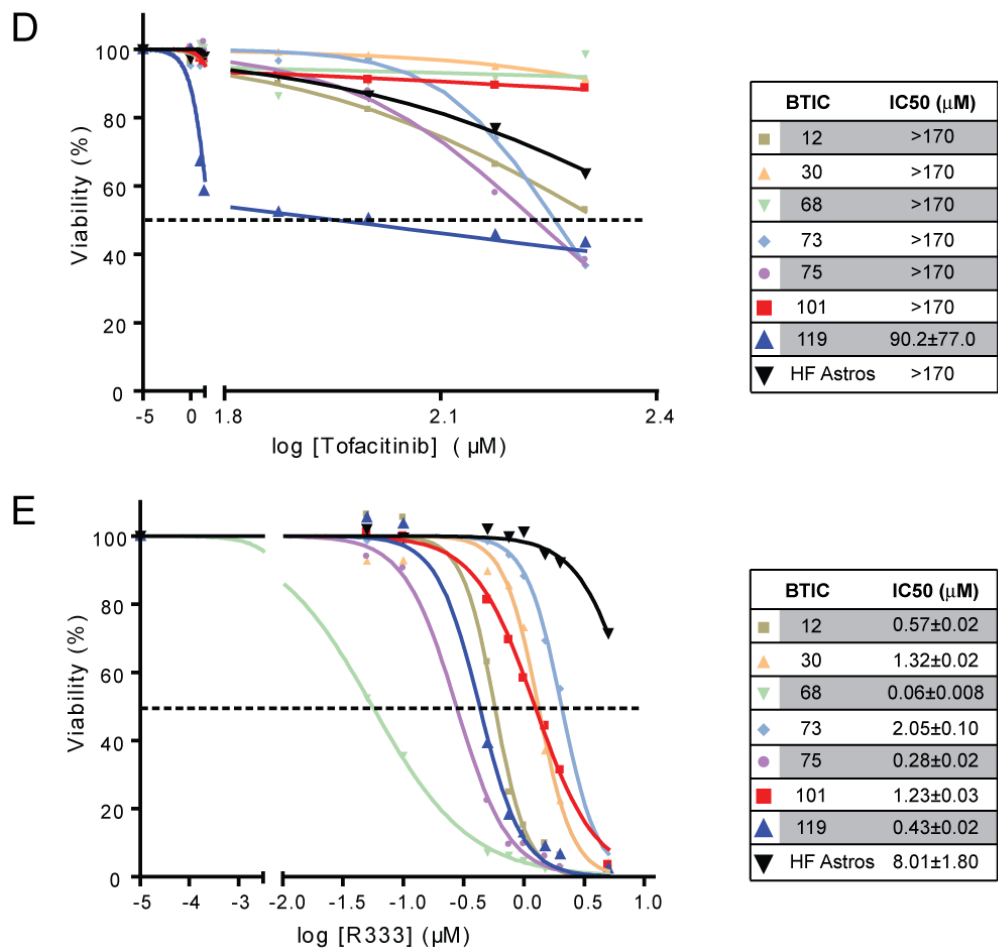


**Figure 8. BTIC lines show varied sensitivity to different JAK/STAT3 inhibitors**

*A*, ZM39923 (ZM) potently inhibited BTIC growth with all IC<sub>50</sub> values below 2.5 μM and no effect on the human fetal astrocytes (HF Astros) control. *B*, With Janex-1 most BTSCs did not show a significant response until concentrations over 20 μM. The IC<sub>50</sub> value for the HF Astros was over 170 μM. *C*, BTIC sensitivity to TCS21311 was widely variable with IC<sub>50</sub> values ranging from 1.13 to 19.19 μM. *D*, Tofacitinib was not effective at inhibiting BTSC growth. *E*, R333 was extremely potent, with most IC<sub>50</sub> values well below 2 μM in BTICs. In contrast, HF Astros had an IC<sub>50</sub> over four times this value.

#### 4.2 ZM and R333 effectively decrease viability in a large panel of BTICs

Of the five compounds tested, the most clearly effective were ZM and R333. These two demonstrated efficacy against all seven of the BTIC lines screened and had IC<sub>50</sub> values well below that of the HFA controls. To better evaluate their efficacy, both compounds were moved on to secondary validation on a panel of 22 BTIC lines (**Table 1**).

The same range of doses used in preliminary screens was replicated in the expanded screen. With ZM, five lines showed a statistically significant response at 0.5  $\mu$ M versus DMSO ( $p < 0.01$ , Student's t-test), resulting in decreases in viability between 15-42%. At 1  $\mu$ M, 9/22 lines were below 50% viable and when increased to 2  $\mu$ M, 16/22 lines were less than 50% viable with most well below 10% ( $p < 0.01$ , Student's t-test; **Figure 9A**). There did not appear to be a correlation between drug sensitivity and specific molecular alterations in BTICs.

Of the BTICs exposed to R333, 10/22 lines were less than 50% viable with only a 0.5  $\mu$ M dose ( $p < 0.01$ , Student's t-test). At 1  $\mu$ M, 18/22 lines were below 50% viability with 10/18 of these lines below 20% viable ( $p < 0.01$ , Student's t-test; **Figure 9B**). When the concentration was increased to 2  $\mu$ M, all tested BTIC lines, with the exception of BT073, were less than 25% viable with most well below 10% viable ( $p < 0.01$ , Student's t-test). Thus, it did not appear that differential *EGFR/PTEN/TP53* mutational states affected R333-mediated JAK/STAT3 inhibition. Additionally, at the higher concentrations of

A

BTIC Line	ZM ( $\mu\text{M}$ )		
	0.5	1	2
12	97.9	93.7*	65.3*
25	101.9	102.0	101.3
30	102.8	93.1	51.9*
42	100.5	99.4	99.1
48	85.8*	48.8*	3.9*
53	77.4*	30.7*	2.6*
54	87.6	23.8*	5.3*
63	57.9*	24.7*	3.9*
68	91.3	65.9*	6.3*
73	98.1	97.5	76.9
75	98.2	56.9*	4.9*
84	97.5	66.7*	9.1*
88	90.7	39.6*	7.7*
89	78.4*	23.2*	3.2*
90	87.9	14.6*	4.1*
92	71.4*	13.1*	2.9*
101	101.9	101.0	74.9
108	96.5	81.0*	11.1*
119	98.2	95.2	26.5*
126	97.0	75.9	44.5*
143	64.2	66.0*	19.4*
147	85.8	12.3*	3.2*
HFA	107.4	107.0	107.1

B

BTIC Line	R333 ( $\mu\text{M}$ )		
	0.5	1	2
12	63.1*	15.2*	6.3*
25	90.6*	76.5*	10.6*
30	89.7*	73.2*	22.5*
42	84.0	35.9*	12.5*
48	68.8*	47.2*	3.5*
53	39.2*	30.7*	6.2*
54	12.9*	8.7*	4.1*
63	15.9*	10.6*	7.0*
68	12.1*	7.5*	5.1*
73	98.5	88.3*	55.2*
75	31.6*	17.0*	7.6*
84	74.3*	26.3*	21.3*
88	60.6*	32.6*	19.6*
89	2.8*	2.5*	2.4*
90	7.4*	4.2*	4.0*
92	7.6*	5.9*	4.8*
101	81.2*	58.2*	31.3*
108	49.2*	28.8*	13.9*
119	39.1*	13.0*	6.6*
126	66.4*	9.4*	3.7*
143	64.9*	53.4*	42.9*
147	55.5*	23.9*	9.5*
HFA	102.6	100.1	78.3*

	0-26%
	26-55%
	>55%

**Figure 9. Low micromolar doses of ZM39923 (ZM) and R333 significantly decrease BTIC viability**

Viability was assessed using alamarBlue™ with results displayed as percent of vehicle control. A, ZM significantly decreased the viability of 9/22 BTIC lines at a concentration of 1  $\mu\text{M}$ . When increased to 2  $\mu\text{M}$ , the number of responding lines increased to 17/22. Human fetal astrocyte (HFA) counterscreen controls were not affected by ZM treatment

at any concentration. *B*, 18/22 BTIC lines responded significantly to R333 at a dose of 1  $\mu\text{M}$ , 10 of which already showed dramatic sensitivity at 0.5  $\mu\text{M}$ . With a dose of 2  $\mu\text{M}$ , all but one BTIC line were less than 55% viable with most lines showing viability below 20%. HFA controls were only modestly affected by the higher concentration of R333. (\* denotes statistically significant difference from DMSO;  $p < 0.01$ , Student's t-test)

R333 (2-5 $\mu$ M), mostly cellular debris remained in the wells, suggesting that at this concentration, the drug was largely cytotoxic.

In a side-by-side comparison, R333 was found to be the superior compound. BTICs were sensitive and responded more completely to R333 at lower concentrations. Additionally, R333 was more successful at inhibiting growth in a range of diverse BTICs than ZM. As such, R333 was selected to be carried forward for further *in vitro* testing.

#### **4.3 R333 significantly decreases BTIC clonogenicity**

In addition to measuring the effect of JAK/STAT3 inhibition on BTIC viability, self-renewal capacity was also assessed using the neurosphere assay. In total, 12 diverse BTIC lines from the secondary validation were used. R333 lead to a dose-dependent decrease in the number of spheres formed, with 7/12 lines completely losing sphere-forming capacity at 0.75  $\mu$ M ( $p < 0.01$ , Tukey's test; **Figure 10A,C**). At 1  $\mu$ M, sphere forming ability was practically ablated in all tested lines ( $p < 0.01$ , Tukey's test; **Figure 10B,D**).

#### **4.4 R333 does not attenuate BTIC sensitivity to TMZ**

TMZ is currently the cornerstone of GBM chemotherapy. As such, novel drugs will likely be tested as adjuvants to this regimen or in TMZ-failed patients. To evaluate BTIC sensitivity to the combination of TMZ and R333, a clinically relevant dose of TMZ (10



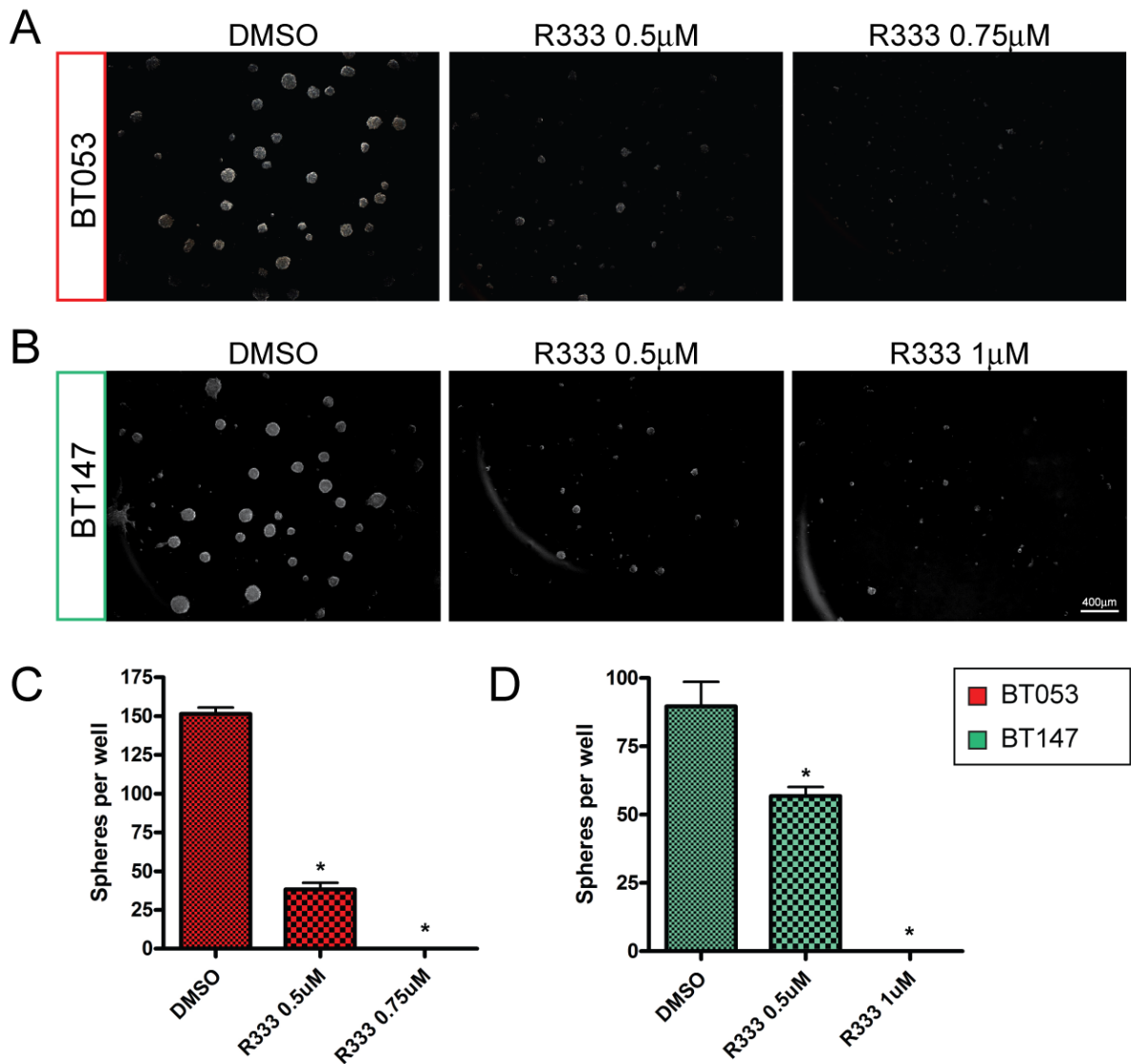


**Figure 10. R333 effectively decreases BTIC clonogenicity**

A,C, In BT053, R333 significantly impaired sphere formation at 0.5 µM and completely abolished sphere forming ability at 0.75 µM ( $p < 0.001$ , Tukey's test). B,D, In BT147, 0.5 µM R333 was also significantly effective in impairing clonogenicity. At 1 µM, sphere forming ability was completely ablated in this line ( $p < 0.001$ , Tukey's test). (\* denotes statistically significant difference from DMSO).

$\mu\text{g/mL}$ ; [101]) was used with a 2  $\mu\text{M}$  dose of R333. A total of 12 BTIC lines with different *MGMT* methylation statuses were tested. Five of the lines were *MGMT* methylated and 4/5 were significantly sensitive to TMZ ( $p < 0.01$ , Tukey's test). When treated together with 2  $\mu\text{M}$  R333, viability was dramatically decreased to a level that was equal to or less than that observed with TMZ treatment alone (**Figure 11A**). In BT143, an *MGMT* methylated line resistant to TMZ due to mutations in the mismatch repair gene *MSH6* (unpublished data), R333 or combination R333+TMZ proved to be more effective than TMZ alone (data not shown). The remaining seven tested BTIC lines were all *MGMT* unmethylated. Although they were all largely resistant to TMZ, all seven lines responded to R333 and R333+TMZ (**Figure 11B**). When R333 and TMZ were tested on HFAs, neither agent alone or in combination significantly reduced viability relative to DMSO vehicle control (**Figure 11C**). Finally, it is interesting to note that in two lines, BT119 and BT126, the combination of a lower 0.5  $\mu\text{M}$  dose of R333, which did not completely ablate BTIC growth on its own, with TMZ resulted in a significantly greater effect than with either agent alone ( $p < 0.01$ , Tukey's test; **Figure 11D,E**). As such, R333 and TMZ may act in a synergistic or additive manner in some cases.

#### **4.5 R333 inhibits STAT3 with minimal effects on other signalling pathways**

In order to avoid the significant off-target toxicity in other tissues that would result from inhibiting other kinases, the ideal JAK/STAT3 inhibitor needs also to be highly specific, in addition to being highly potent. At a dose of 0.5  $\mu\text{M}$ , R333 was able to strongly impair STAT3 activation in the three BTIC lines tested, as demonstrated by the decrease in

STAT3 phosphorylation on tyrosine residue 705 (representative data with BT147 shown; **Figure 12**). Moreover, at this concentration, R333 did not impact other signalling pathways, as indicated by unchanged levels of p-Erk 1/2 T202/T204, p-STAT3 S727, p-Akt S473, and p-S6 S240/244 (**Figure 12A**). Evidence of on-target inhibition of STAT3 activity was apparent in a decrease in the level of cyclin D1, a downstream transcriptional target of STAT3 (**Figure 12B**). Additionally, STAT3 inhibition with R333 led to an increased level of cleaved PARP, a marker of cells undergoing apoptosis, relative to DMSO control, at both two and 24 hours post-treatment (**Figure 12C**).

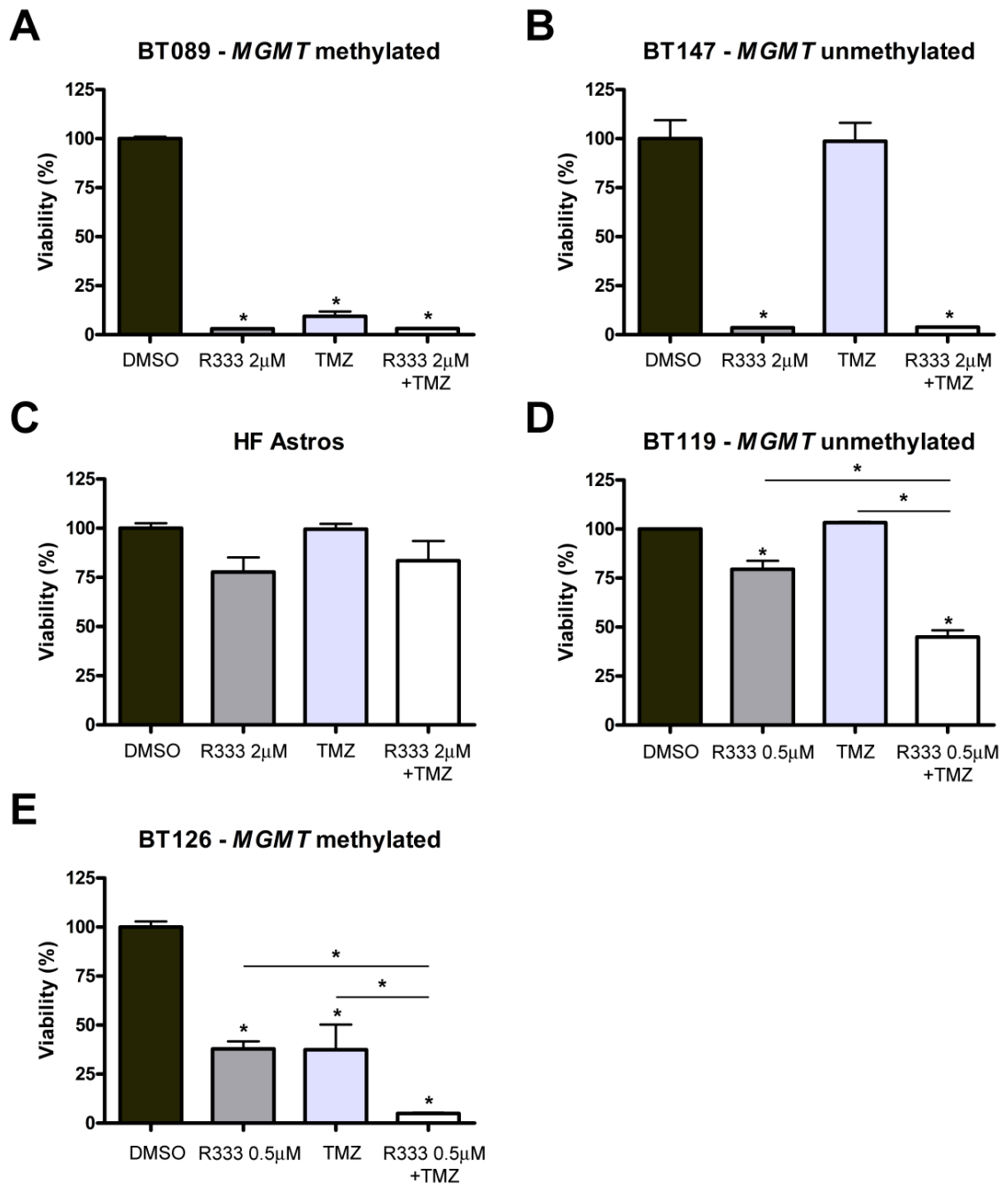


**Figure 11. R333 does not adversely affect BTIC sensitivity to temozolomide (TMZ)**

A, BT089 is an *MGMT* promoter methylated line sensitive to TMZ. Treatment with 2  $\mu$ M R333 did not attenuate TMZ sensitivity. B, In BT147, an *MGMT* promoter unmethylated

line resistant to TMZ, BTIC growth was inhibited by R333 alone and this effect was not affected by the addition of TMZ. *C*, Human fetal astrocytes (HF Astros) were used as a counterscreen control and demonstrated that combining R333 with TMZ was not any more toxic than either agent alone. *D,E*, In BT119 and BT126, the combination of a 0.5  $\mu$ M dose of R333 and TMZ resulted in a decrease in BTIC viability significantly greater than either agent alone. (\* denotes  $p < 0.01$  versus DMSO control or as indicated, Tukey's test).

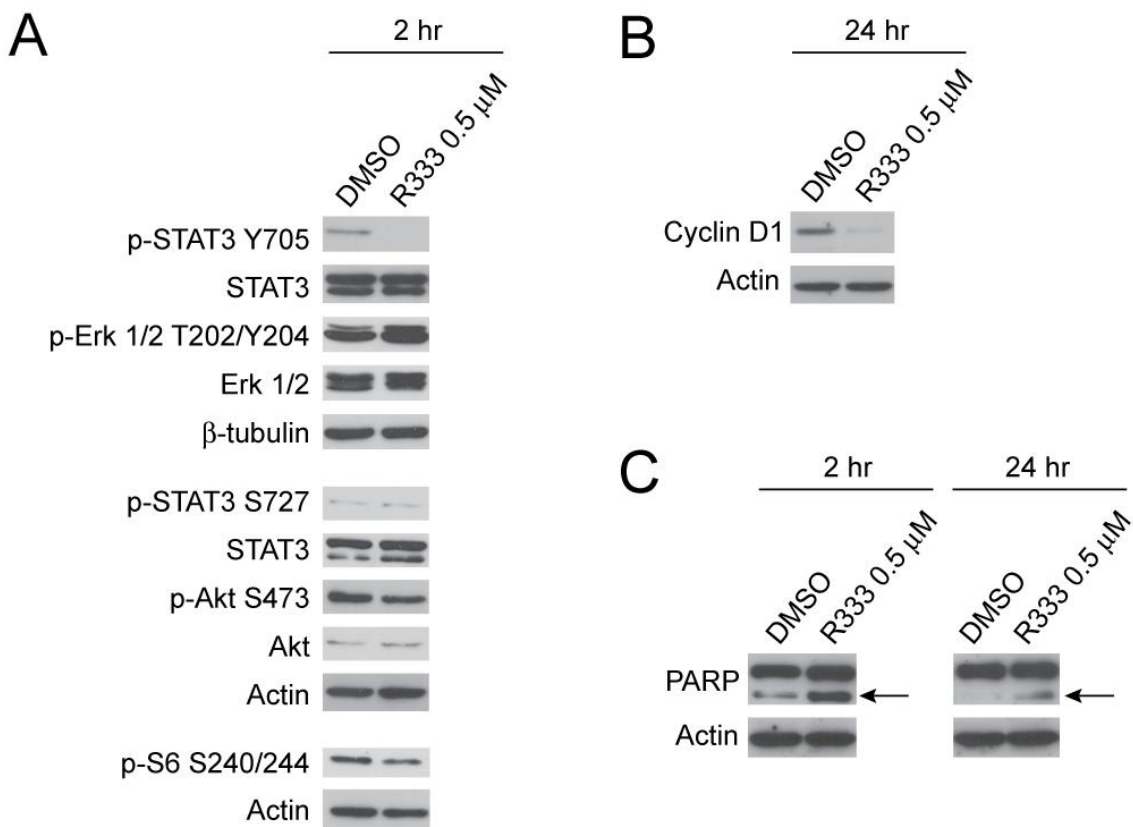


**Figure 12. R333 specifically inhibits STAT3 with negligible effects on other signalling pathways**

A, Two hours following exposure to 0.5  $\mu$ M R333, STAT3 activation by phosphorylation of tyrosine 705 (p-STAT3 Y705) was completely inhibited in BT147. Changes in other signalling pathways as assayed by p-Erk 1/2 T202/Y204, p-STAT3 S727, p-Akt S473, and p-S6 S240/244 levels were not observed. B, On-target inhibition of STAT3 resulted in decreased expression of the downstream transcriptional target cyclin D1. C, 0.5  $\mu$ M R333 increased the expression of cleaved PARP (arrow), a marker of cells undergoing apoptosis, relative to DMSO controls.

#### **4.6 R348 is metabolized to R333 *in vivo*, which accumulates to relevant concentrations in the brain**

We collaborated with the Ontario Institute for Cancer Research, to evaluate the pharmacokinetic properties of R333 and its prodrug, R348. As outlined in *Materials and Methods*, R348 was given to mice at 25, 50 and 100 mg/kg and collected at 0.5 and 5 hour (hr) time points. At the 25 mg/kg dose, the plasma concentration of R348 significantly decreased between 0.5 and 5 hrs and no active metabolite (R333) was observed at the later time point. At both the 50 and 100 mg/kg doses, the concentration of the prodrug went from approximately 12  $\mu\text{M}$  at 0.5 hr to 6  $\mu\text{M}$  at 5 hr. The concentration of the active metabolite at the later time point for these doses was 1 and 3.5  $\mu\text{M}$ , respectively (**Figure 13**).

The lack of significant difference in plasma prodrug concentrations at the 0.5 and 5 hr time points between the 50 and 100 mg/kg doses (**Figure 13A**) was sufficient evidence to pursue the lower dose for subsequent experimentation. LC-MS analysis of brains from mice injected with this dose demonstrated penetration of the blood-brain barrier and accumulation of R333 to 0.5  $\mu\text{M}$  at both 0.5 and 5 hr time points. No R348 was detected at either time point indicating that the prodrug was metabolized to the active form.

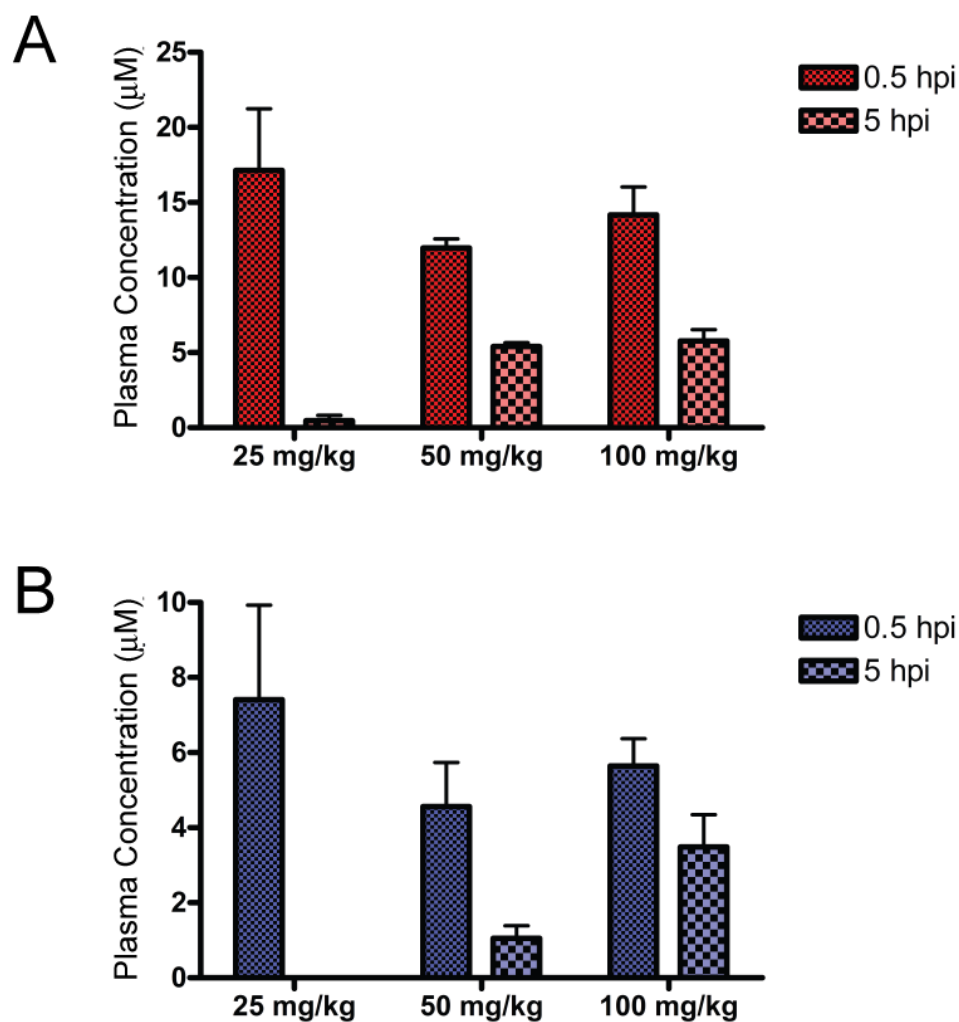


**Figure 13. Administration of R348 leads to the accumulation of R333**

25, 50 and 100 mg/kg doses of R348 were administered i.p. and assayed 0.5 and 5 hours post injection (hpi). *A*, At the 0.5 hpi time point, the plasma concentration of R348 (red) was similar over the three doses. At 5 hpi, the 50 and 100 mg/kg doses resulted in the detection of R348 at 5.4 and 5.8 µM, respectively. *B*, The plasma concentration of R333 (indigo) was comparable at 5 hpi between the three doses. At 5 hpi, the plasma concentration of R333 seemed to increase dose dependently. Data courtesy A. Aman.



#### 4.7 Systemic R348-treatment reduces STAT3 activation *in vivo*

Promising *in vitro* data combined with favourable pharmacokinetic properties were convincing evidence to further pursue R348 *in vivo*, using an orthotopic BTIC xenograft model. For this purpose, an aggressive BTIC line with previously demonstrated tumourigenic capacity was selected [36]. BT147 is derived from a recurrent GBM and is in itself an *MGMT* unmethylated, TMZ-resistant line, with EGFRvIII and mutation of both *PTEN* and *TP53*. When implanted into the brains of NOD SCID mice, this line initiates measurable tumours as early as seven days post-implantation.

To evaluate targeted inhibition of STAT3, six mice were xenografted and started receiving vehicle (n=3) or 50 mg/kg R348 (n=3) seven days post-implantation. Vehicle or R348 was administered on days 7, 9, 12, 14, and 16 to correspond with a thrice weekly treatment regimen and mice were sacrificed two hours following the last dose. On gross histological assessment, the tumours in both vehicle and R348-treated mice contained large cells with hyperchromatic nuclei, forming a dense mass in the deep grey matter (**Figure 14A**). The migration of single cells throughout the parenchyma and along white matter tracts, especially the corpus callosum, was also evident. Tumours in both groups did not display extensive neovascularization. To detect activated STAT3, an antibody specific to STAT3 phosphorylated on tyrosine residue 705 (p-STAT3 Y705) was used. As expected, BT147 expressed endogenous p-STAT3 Y705, which was localized in the nucleus. Positive staining for p-STAT3 Y705 was apparent in vehicle and R348-treated brains. Qualitatively, R348-treated animals appeared to have fewer p-STAT3 Y705

positive cells compared to vehicle counterparts, suggesting that systemic administration of R348 can inhibit JAK/STAT3 signalling within intracranial tumour cells (**Figure 14B**).

#### **4.8 R348 provides a significant benefit to overall median survival**

After meeting the requirements for stable pharmacokinetics and demonstrating targeted STAT3 inhibition, the final stage of validation involved determining if R348 could provide therapeutic benefit to BTIC bearing mice. Fourteen mice were xenografted with  $10^5$  BT147 cells each, randomized to drug (n=8) and vehicle (n=6) cohorts and started on their respective treatments on day 7 (**Figure 15A**). Within the vehicle cohort, all animals tolerated the 50% PEG 300 in water well. The first control mouse was found dead unexpectedly early on day 18; however, necropsy revealed tumour growth on the surface of the brain. Thus, this mouse was labelled an outlier and removed from subsequent analysis. Progressively, vehicle mice began exhibiting characteristic signs of a critically increasing tumour burden including decreased grooming, weight loss and hunching. The remaining vehicle mice became ill, necessitating sacrifice on days 32 (1 mouse), 37 (3 mice) and 39 (2 mice). The overall median survival for the vehicle cohort was 37 days (**Figure 15B**).

The R348-treated mice tolerated the 40 mg/kg dose and thrice weekly regimen well. During the course of treatment (day 7 through to day 37), there were no indications to

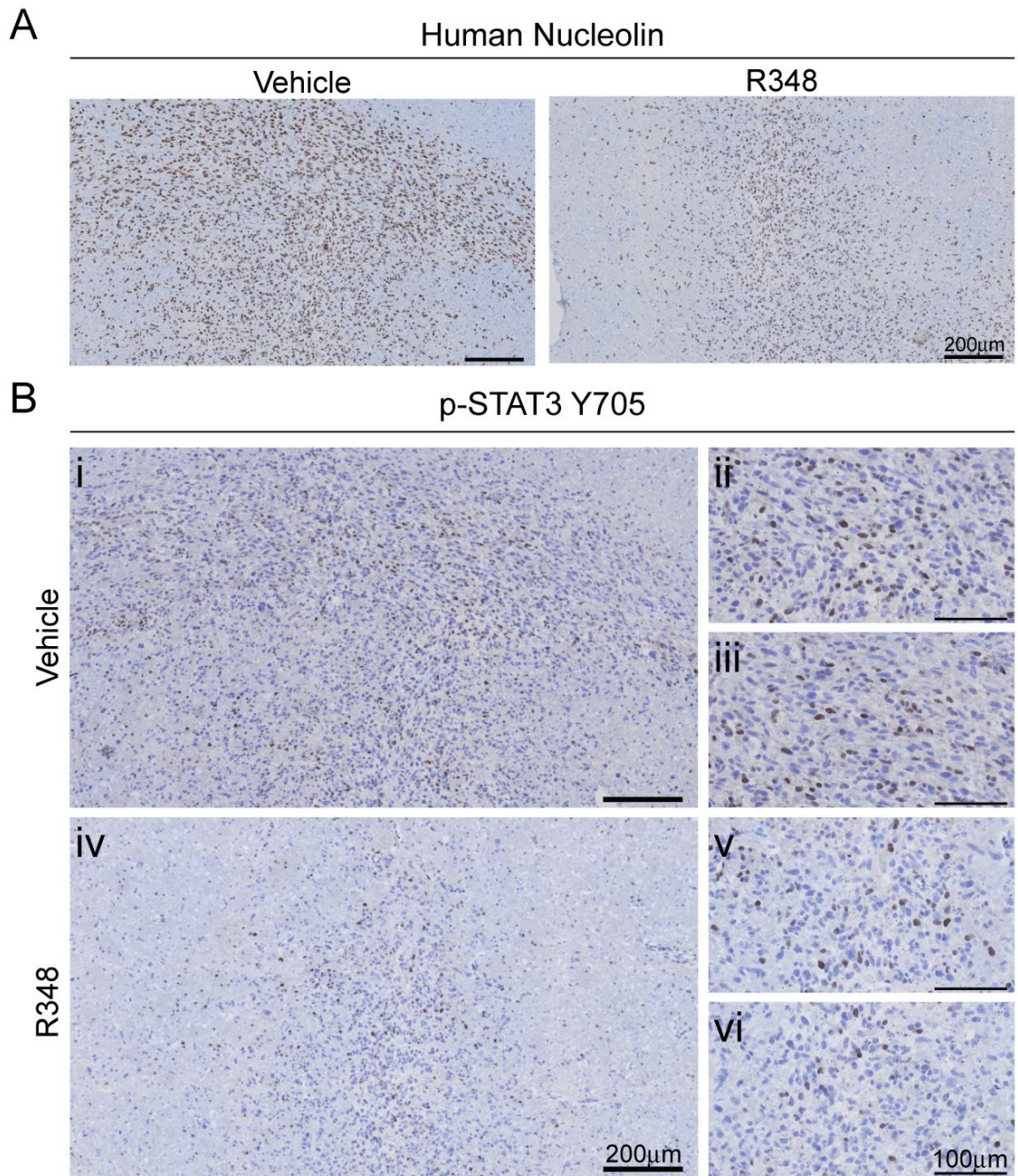


**Figure 14. Systemic R348 treatment reduces JAK/STAT3 signalling *in vivo***

A, Immunohistochemical staining with human nucleolin identified tumours generated by xenografted BT147 cells in the brains of NOD SCID mice treated systemically with vehicle or R348. B, *In vivo*, BT147 cells endogenously expressed activated STAT3 as

demonstrated by positive staining for STAT3 phosphorylated on tyrosine residue 705 (p-STAT3 Y705, *i-iii*). Although p-STAT3 Y705 expression was variable, a marked qualitative decrease in phosphorylation was apparent in the R348-treated brains (*iv-vi*) relative to the vehicle-treated cohort. Representative staining from one vehicle and one R348-treated mouse shown.

suggest drug toxicity. Signs of illness and weight loss began on day 40. Sacrifice was necessitated on days 44 (1 mouse), 49 (5 mice), 53 (1 mouse), and 59 (1 mouse). The overall median survival for the drug-treated group was 49 days (**Figure 15B**). Kaplan-Meier analysis showed that there was a statistically significant difference in survival between the two groups (logrank test,  $p=0.0001$ ).

Additional Kaplan-Meier survival studies using BT147 were also pursued, with the concentration of R348 increased from 40 to 50 mg/kg, as this was the concentration evaluated in pharmacokinetic analyses. In one of the studies, drug administration started on day 14 with a dosing regimen of five consecutive days followed by two days off to a total of 17 doses. While there appeared to be no benefit to survival in this study, the results were potentially confounded by the later start of treatment and the increased dose and frequency of drug administration. In a second study more closely resembling the dosing regimen and start date post-xenograft in the first study, a statistically significant although more modest (40 days in vehicle vs. 44 days in R348-treated; logrank test,  $p=0.03$ ) increase in overall median survival was again achieved.

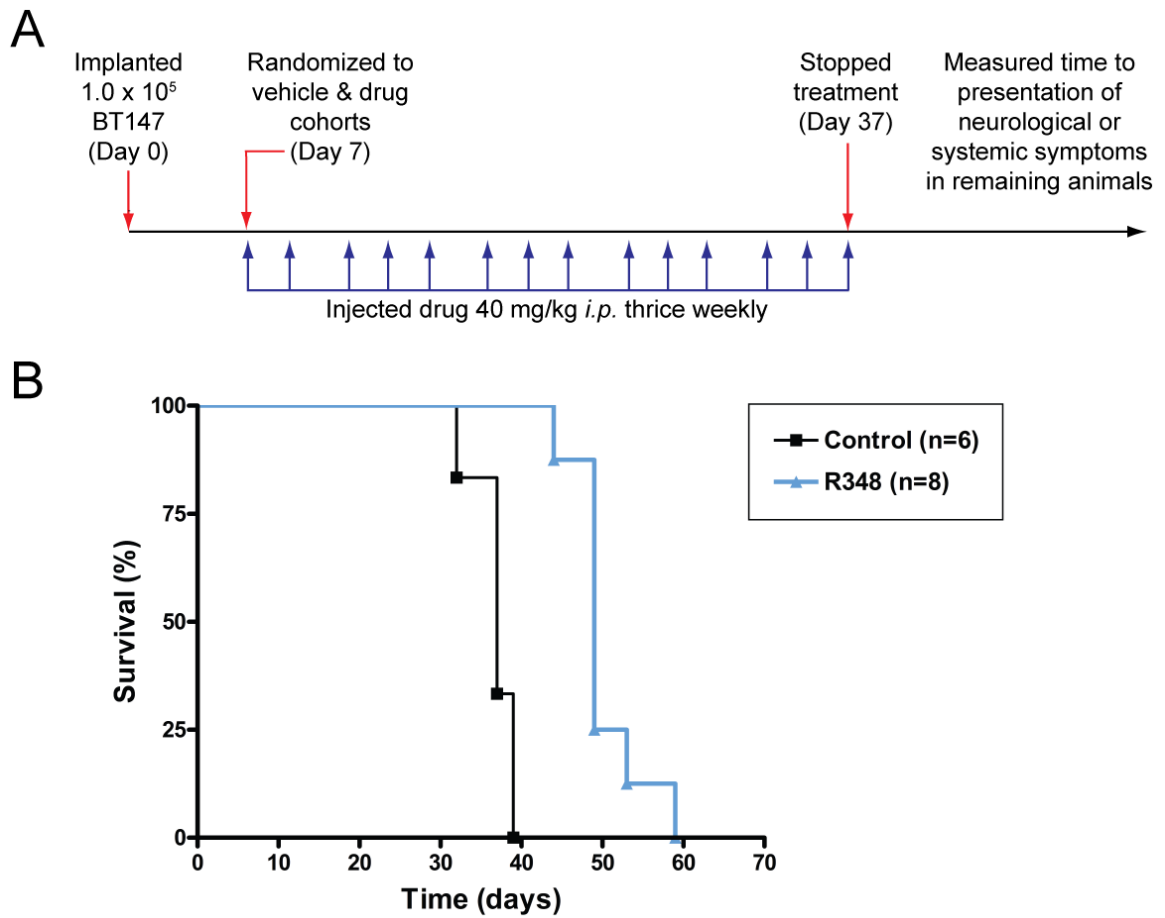


**Figure 15. Systemic administration of R348 slows tumour progression in BT147 orthotopic xenografts**

A, Schematic illustrating the treatment regimen for *in vivo* analysis of R348, the prodrug form of R333. B, Kaplan-Meier analysis demonstrated that R348 provided a significant survival benefit. Overall median survival increased from 37 days in the vehicle cohort to 49 days in the R348-treated cohort ( $p=0.0001$ , logrank test).

## 5. DISCUSSION

The central objective of this work was to identify a JAK/STAT3 inhibitor that would meet particular *in vitro* qualities to carry forward into a preclinical *in vivo* setting. Two strategies were employed to identify potential compounds. The first involved mining existing data generated by high throughput screening performed as part of an existing collaborative study between the Weiss and Kaplan groups. Due to its rapidity and the extensive collection of drug libraries available, high throughput screening is an invaluable tool for identifying potentially useful compounds. However, the breadth of testable drugs also contributes to one of the complications of high throughput strategies: selecting a place to begin. In this case, through an existing body of work by others and our group, the target of interest – the JAK/STAT3 signalling pathway – was defined, enabling the results of the HTS to be narrowed to a particular set of compounds. Then, within the range of JAK/STAT3 inhibitors screened, it was possible to identify those that were most effective to move ahead for further validation. The second approach was less stringent and was based solely on selecting JAK/STAT3 inhibitors that were novel for GBM, but already in clinical trials for other indications. This approach was attractive primarily because such drugs would have already undergone extensive testing in phase I, II, or III trials, allowing for expedited translation into the clinic if their efficacy could be demonstrated for GBM. Here, the use of both strategies resulted in the identification of a novel set of JAK/STAT3 inhibitors that could be moved on to primary screening and subsequent secondary validation in BTICs.

The two compounds initially identified in the HTS were reported to have significant affinity for JAK3, suggesting that JAK3 may play an important role in JAK/STAT signalling in GBM. JAK3 is an attractive target as its expression is more limited in the body and unlike JAK2, its activity is not critically important for hematopoiesis. Therefore, a number of compounds with affinity primarily for JAK3 were selected to try and maximize STAT3 inhibition while minimizing side effects in other normal tissues. Tofacitinib was touted as the most specific of the compounds tested for JAK3, but appeared to be the least effective against diverse BTIC lines. In contrast, drugs such as ZM and R333, which more broadly inhibited members of the JAK family, were found to be more widely effective. These data suggest that singly targeting JAK3 may not be sufficient to effectively decrease BTIC proliferation *in vitro*. It may be that JAK3 is not primarily responsible for STAT3 signalling in BTICs or multiple JAK family members operate upstream of STAT3 in a semi-redundant fashion in BTICs. Characterization of the expression of different JAK family members was outside of the scope of this thesis. However, in the future, doing so would help elucidate this point and perhaps guide further refinement in drug design to selectively inhibit only the JAK family members responsible for STAT3 activity. In this way, compounds that inhibit the right combination or balance of JAK family members may be the most effective in broadly targeting BTICs. At the same time, this strategy may also avoid the potentially limiting toxicity of concentrated blockade of a single JAK family member, as has been the case for JAK2 inhibitors like Cucurbitacin or WP1066 [36].



Limited toxicity aside, the most obvious feature of a promising novel JAK/STAT3 inhibitor was demonstrated potency in a large panel of molecularly diverse BTIC lines. Given this criterion, it was almost immediately possible to identify R333 as the superior of the compounds evaluated. The  $IC_{50}$  values determined in the panel of 22 BTIC lines ranged from 50 nM to 1.30  $\mu$ M excluding one highly aggressive line (BT073) possessing an  $IC_{50}$  of 2.05  $\mu$ M. Achieving efficacy at low doses was especially important as comparable doses need to be achieved *in vivo* to be physiologically relevant.

Additionally, the  $IC_{50}$  range in the BTICs was in stark contrast to the  $IC_{50}$  for human fetal astrocytes, which was approximately 4.5 fold greater. This therapeutic index was promising as it suggested the possibility of a window without unacceptable dose-limiting toxicity. Perhaps the most striking result of *in vitro* validation was the consistency with which R333 controlled BTIC growth. In all of the assays and tested BTIC lines, R333 seemed to be universally effective. This is in agreement with previous work using JAK2 inhibitors [36] and further reaffirms the important role of JAK/STAT3 signalling in BTIC survival and proliferation. However, whether the universality would apply to actual GBM patients is uncertain. As mentioned in the Introduction, the collection of BTIC lines generated by the Weiss group possesses the genetic, molecular and phenotypic heterogeneity of the GBMs from which they were derived. The lab has generated lines with genomic features characteristic of the proneural (*IDH1* mutation), classical (*EGFR* mutation or vIII) and mesenchymal (STAT3, decreased NF1 expression) subtypes. As *IDH1* mutant lines were not included in the evaluation of R333, it is possible the results obtained here are only reflective of classical and mesenchymal GBMs. Even if this were the case, these two subtypes together account for more than half of GBM patients [12],

which would still mean targeting a larger proportion of likely responders than the 21-40% of *MGMT* methylated GBMs that TMZ does [1, 5, 9].

Among the panel of BTICs tested were lines derived from recurrent or *MGMT* unmethylated GBMs. Despite being resistant to TMZ, these lines were sensitive to R333. In one case, BT119 was only modestly sensitive to R333 at a dose of 0.5  $\mu$ M; however when combined with TMZ, this combination proved to be more effective than either agent alone, suggesting the prospect that R333 may augment TMZ sensitivity in minimally responsive lines. Importantly, in all lines responsive to TMZ, R333 did not attenuate sensitivity. As such, R333 may be a useful adjuvant or salvage therapy for patients whose disease has recurred with acquired resistance to TMZ.

Despite promising *in vitro* results, the crux of many of the JAK/STAT3 inhibitors tested to date has been *in vivo* performance. Here, R348, the prodrug form of R333, was found to be fairly stable, allowing for the detection of R333 at a relevant concentration in both the plasma and brains of non-tumour bearing mice. These properties mean R333 has the potential to accumulate to a therapeutic dose throughout the entire tumour, including distant disseminated tumour cells behind an intact BBB. In line with this, R348-treatment in tumour-bearing mice appeared to reduce the extent of p-STAT3 Y705 positive staining (**Figure 14**). While this may be the case, it cannot be unequivocally concluded that systemic administration of R348 inhibited JAK/STAT3 signalling *in vivo*. A caveat of the immunohistochemical staining performed here is the potential of also staining host cells that have activated STAT3. In the future, double labelling with anti-human nucleolin and

p-STAT3 Y705 will be required to exclude this possibility. In addition, quantification at several different stereological levels will reduce sampling error and make it possible to unequivocally demonstrate STAT3 inhibition and better assess its extent throughout the tumour. Nevertheless, a five-week regimen of R348 was not only well tolerated by tumour-bearing mice, but led to a significant increase in median survival. This was especially impressive considering the highly aggressive nature of BT147, the *MGMT* unmethylated *EGFR/PTEN/TP53* mutant used for xenograft experiments.

Although beneficial during the course of treatment, the cessation of R348 was followed by the precipitous deterioration of these mice. Together with the results of the *in vivo* targeting assessment, this suggests that R348 can hold the tumour in check but not efficiently kill all of the cells to cure the disease – after all, only as few as 10 BTICs have been shown to have the ability to initiate a tumour [28]. This begs the question as to whether a continuous, long-term treatment regimen would be more successful. Here, mice were treated for five weeks and only three times weekly. As R333/R348 is an ATP-competitive inhibitor, days in which mice were not treated may have been opportunities for residual BTICs to grow and proliferate. When a continuous dosing regimen was applied in a second survival study, there did not appear to be any benefit. Mice in the R348-treated cohort were in as equally poor condition as the vehicle-treated mice and had a similar median survival. A potential explanation for the lack of benefit may be the delayed start of treatment. When treatment began on day 14, the increased tumour burden may have already been too high to achieve significant response by chemotherapy alone. The lack of benefit may also have been a result of the more intense treatment regimen.

Although there was no observed toxicity with the thrice weekly regimen, the five consecutive injections at a higher concentration may have been less well tolerated. Nonetheless, the feasibility of long term, continuous dosing with this compound has been previously demonstrated. In the treatment of a murine model of psoriasis, animals were given 40, 80 or 120 mg/kg doses of R348 daily for over 6 weeks. Even at the highest dose, mice did not develop any of the adverse events typically associated with JAK inhibition [99]. Similar tolerability was also observed in a study evaluating the use of R348 to prevent airway allograft rejection [102]. In this study, Lewis rats were treated daily for 28 days with 10, 20, 40, and 80 mg/kg doses and R348 was well tolerated up to 40 mg/kg. Taken together, these studies provide proof for the tolerability of daily R348 administration.

While daily R348 treatment may be tolerated for 6 weeks in rodents, long term JAK/STAT3 inhibition in humans is not without potential side effects. If R348 does inhibit JAK2 to some degree, long term dosing may incur the therapy-related anemia and thrombocytopenia seen with JAK2 inhibitors in clinical trials [103]. Careful monitoring will thus be essential, as in most other chemotherapy regimens, to minimize and treat any potential side effects. Chronic R348 administration also has the potential to significantly impact immune function. The link between drugs that alter immune function and the risk of reactivation of latent infections, decreased ability to fight off new infections and increased risk of certain neoplasms is well established [104, 105]. However, given the universally poor prognosis for GBM, achieving improved tumour control would almost certainly outweigh these risks.

## 6. CONCLUSION

In the last few decades, our ever-expanding understanding of the biology of GBM has provided substantial insight into the molecular heterogeneity underlying this disease. Great advances have also been made in strategies for imaging, surgical resection and radio- and chemotherapies. Yet, in spite of this progress, the prognosis for GBM remains very poor with patient outcome still being measured in months.

We, and others, have shown the JAK/STAT3 pathway to be a major oncogenic signalling hub for BTICs that is amenable to therapeutic targeting. This work demonstrates that R333/348 possess a number of key pharmacologic properties, including on-target inhibition at low micromolar doses and broad efficacy against diverse BTICs. Perhaps most importantly, this drug demonstrates BBB permeability and *in vivo* efficacy with systemic administration. Therefore, R348 is a very promising compound worthy of further *in vivo* validation, to confirm efficacy with additional BTIC lines and evaluate whether durable tumour control may be achieved with more frequent, long-term administration. Given that R348 is already approved for Phase I and II trials in dry eye and discoid lupus erythematosus, progression to an early phase trial for GBM would be a reasonable and feasible endeavour, should further preclinical evaluation continue to yield consistently positive results. As such, compounds such as R348 may have the potential to do for GBM what Gleevec has done in CML – convert a fatal disease into a chronic condition that can be managed medically.

## 7. REFERENCES

1. Louis DN, Ohgaki H, Wiestler OD, Cavenee WK, editors. WHO classification of tumours of the central nervous system. Lyon: IARC; 2007.
2. Wen PY, Kesari S. Malignant gliomas in adults. *N Engl J Med*. 2008 Jul 31;359(5):492-507.
3. Jemal A, Siegel R, Xu J, Ward E. Cancer statistics, 2010. *CA Cancer J Clin*. 2010 Sep-Oct;60(5):277-300.
4. Walker MD, Alexander E, Jr., Hunt WE, MacCarty CS, Mahaley MS, Jr., Mealey J, Jr., Norrell HA, Owens G, Ransohoff J, Wilson CB, Gehan EA, Strike TA. Evaluation of BCNU and/or radiotherapy in the treatment of anaplastic gliomas. A cooperative clinical trial. *J Neurosurg*. 1978 Sep;49(3):333-343.
5. Hegi ME, Diserens AC, Gorlia T, Hamou MF, de Tribolet N, Weller M, Kros JM, Hainfellner JA, Mason W, Mariani L, Bromberg JE, Hau P, Mirimanoff RO, Cairncross JG, Janzer RC, Stupp R. MGMT gene silencing and benefit from temozolomide in glioblastoma. *N Engl J Med*. 2005 Mar 10;352(10):997-1003.
6. Ohgaki H, Kleihues P. Genetic pathways to primary and secondary glioblastoma. *Am J Pathol*. 2007 May;170(5):1445-1453.
7. Ohgaki H, Dessen P, Jourde B, Horstmann S, Nishikawa T, Di Patre PL, Burkhard C, Schuler D, Probst-Hensch NM, Maiorka PC, Baeza N, Pisani P, Yonekawa Y, Yasargil MG, Lutolf UM, Kleihues P. Genetic pathways to glioblastoma: a population-based study. *Cancer Res*. 2004 Oct 1;64(19):6892-6899.

8. Stechishin ODM. Molecular therapeutics for glioblastoma brain tumor stem cells. Calgary, AB, Canada: University of Calgary; 2011.
9. Cancer Genome Atlas Research N. Comprehensive genomic characterization defines human glioblastoma genes and core pathways. *Nature*. 2008 Oct 23;455(7216):1061-1068.
10. Parsons DW, Jones S, Zhang X, Lin JC, Leary RJ, Angenendt P, Mankoo P, Carter H, Siu IM, Gallia GL, Olivi A, McLendon R, Rasheed BA, Keir S, Nikolskaya T, Nikolsky Y, Busam DA, Tekleab H, Diaz LA, Jr., Hartigan J, Smith DR, Strausberg RL, Marie SK, Shinjo SM, Yan H, Riggins GJ, Bigner DD, Karchin R, Papadopoulos N, Parmigiani G, Vogelstein B, Velculescu VE, Kinzler KW. An integrated genomic analysis of human glioblastoma multiforme. *Science*. 2008 Sep 26;321(5897):1807-1812.
11. Phillips HS, Kharbanda S, Chen R, Forrest WF, Soriano RH, Wu TD, Misra A, Nigro JM, Colman H, Soroceanu L, Williams PM, Modrusan Z, Feuerstein BG, Aldape K. Molecular subclasses of high-grade glioma predict prognosis, delineate a pattern of disease progression, and resemble stages in neurogenesis. *Cancer Cell*. 2006 Mar;9(3):157-173.
12. Verhaak RG HK, Purdom E, Wang V, Qi Y, Wilkerson MD, Miller CR, Ding L, Golub T, Mesirov JP, Alexe G, Lawrence M, O'Kelly M, Tamayo P, Weir BA, Gabriel S, Winckler W, Gupta S, Jakkula L, Feiler HS, Hodgson JG, James CD, Sarkaria JN, Brennan C, Kahn A, Spellman PT, Wilson RK, Speed TP, Gray JW, Meyerson M, Getz G, Perou CM, Hayes DN, Cancer Genome Atlas Research Network. Integrated genomic analysis identifies clinically relevant

- subtypes of glioblastoma characterized by abnormalities in PDGFRA, IDH1, EGFR, and NF1. *Cancer Cell*. 2010;17(1):98-110.
13. Carro MS, Lim WK, Alvarez MJ, Bollo RJ, Zhao X, Snyder EY, Sulman EP, Anne SL, Doetsch F, Colman H, Lasorella A, Aldape K, Califano A, Iavarone A. The transcriptional network for mesenchymal transformation of brain tumours. *Nature*. 2010 Jan 21;463(7279):318-325.
  14. Spiro T, Liu L, Majka S, Haaga J, Willson JKV, Gerson SL. Temozolomide: The effect of once- and twice-a-day dosing on tumor tissue levels of the DNA repair protein O6-Alkylguanine-DNA-Alkyltransferase. *Clin Cancer Res*. 2001;7:2309-2317.
  15. Esteller M, Garcia-Foncillas J, Andion E, Goodman SN, Hidalgo OF, Vanaclocha V, Baylin SB, Herman JG. Inactivation of the DNA-repair gene MGMT and the clinical response of gliomas to alkylating agents. *N Engl J Med*. 2000 Nov 9;343(19):1350-1354.
  16. Stupp R, Mason WP, van den Bent MJ, Weller M, Fisher B, Taphoorn MJ, Belanger K, Brandes AA, Marosi C, Bogdahn U, Curschmann J, Janzer RC, Ludwin SK, Gorlia T, Allgeier A, Lacombe D, Cairncross JG, Eisenhauer E, Mirimanoff RO, European Organisation for R, Treatment of Cancer Brain T, Radiotherapy G, National Cancer Institute of Canada Clinical Trials G. Radiotherapy plus concomitant and adjuvant temozolomide for glioblastoma. *N Engl J Med*. 2005 Mar 10;352(10):987-996.
  17. Reya T, Morrison SJ, Clarke MF, Weissman IL. Stem cells, cancer, and cancer stem cells. *Nature*. 2001 Nov 1;414(6859):105-111.



18. Huntly BJ, Gilliland DG. Leukaemia stem cells and the evolution of cancer-stem-cell research. *Nat Rev Cancer*. 2005 Apr;5(4):311-321.
19. Vermeulen L, de Sousa e Melo F, Richel DJ, Medema JP. The developing cancer stem-cell model: clinical challenges and opportunities. *Lancet Oncol*. 2012 Feb;13(2):e83-89.
20. Bonnet D, Dick JE. Human acute myeloid leukemia is organized as a hierarchy that originates from a primitive hematopoietic cell. *Nature Medicine*. 1997 Jul;3(7):730-737.
21. Nguyen LV, Vanner R, Dirks P, Eaves CJ. Cancer stem cells: an evolving concept. *Nat Rev Cancer*. 2012 Feb;12(2):133-143.
22. Singh SK, Clarke ID, Terasaki M, Bonn VE, Hawkins C, Squire J, Dirks PB. Identification of a cancer stem cell in human brain tumors. *Cancer Res*. 2003 Sep 15;63(18):5821-5828.
23. Galli R, Binda E, Orfanelli U, Cipelletti B, Gritti A, De Vitis S, Fiocco R, Foroni C, Dimeco F, Vescovi A. Isolation and characterization of tumorigenic, stem-like neural precursors from human glioblastoma. *Cancer Res*. 2004 Oct 1;64(19):7011-7021.
24. Yuan X, Curtin J, Xiong Y, Liu G, Waschmann-Hogiu S, Farkas DL, Black KL, Yu JS. Isolation of cancer stem cells from adult glioblastoma multiforme. *Oncogene*. 2005;23(58):9392-9400.
25. Vescovi AL GR, Reynolds BA. Brain tumor stem cells. *Nat Rev Cancer*. 2006;6(6):425-436.

26. Hemmati HD, Nakano I, Lazareff JA, Masterman-Smith M, Geschwind DH, Bronner-Fraser M, Kornblum HI. Cancerous stem cells can arise from pediatric brain tumors. *Proceedings of the National Academy of Sciences of the United States of America*. 2003 Dec 9;100(25):15178-15183.
27. Singh SK, Hawkins C, Clarke ID, Squire JA, Bayani J, Hide T, Henkelman RM, Cusimano MD, Dirks PB. Identification of human brain tumour initiating cells. *Nature*. 2004 Nov 18;432(7015):396-401.
28. Kelly JJ, Stechishin O, Chojnacki A, Lun X, Sun B, Senger DL, Forsyth P, Auer RN, Dunn JF, Cairncross JG, Parney IF, Weiss S. Proliferation of human glioblastoma stem cells occurs independently of exogenous mitogens. *Stem Cells*. 2009 Aug;27(8):1722-1733.
29. Lee J, Kotliarova S, Kotliarov Y, Li AG, Su Q, Donin NM, Pastorino S, Purow BW, Christopher N, Zhang W, Park JK, Fine HA. Tumor stem cells derived from glioblastomas cultured in bFGF and EGF more closely mirror the phenotype and genotype of primary tumors than do serum-cultured cell lines. *Cancer Cell*. 2006 May;9(5):391-403.
30. Liu G, Yuan X, Zeng Z, Tunici P, Ng H, Abdulkadir IR, Lu L, Irvin D, Black KL, Yu JS. Analysis of gene expression and chemoresistance of CD133+ cancer stem cells in glioblastoma. *Mol Cancer*. 2006;5:67.
31. Bleau AM, Hambarzumyan D, Ozawa T, Fomchenko EI, Huse JT, Brennan CW, Holland EC. PTEN/PI3K/Akt pathway regulates the side population phenotype and ABCG2 activity in glioma tumor stem-like cells. *Cell Stem Cell*. 2009 Mar 6;4(3):226-235.

32. Salmaggi A, Boiardi A, Gelati M, Russo A, Calatozzolo C, Ciusani E, Sciacca FL, Ottolina A, Parati EA, La Porta C, Alessandri G, Marras C, Croci D, De Rossi M. Glioblastoma-derived tumorspheres identify a population of tumor stem-like cells with angiogenic potential and enhanced multidrug resistance phenotype. *Glia*. 2006 Dec;54(8):850-860.
33. Bao S, Wu Q, McLendon RE, Hao Y, Shi Q, Hjelmeland AB, Dewhirst MW, Bigner DD, Rich JN. Glioma stem cells promote radioresistance by preferential activation of the DNA damage response. *Nature*. 2006 Dec 7;444(7120):756-760.
34. Stechishin ODM, Luchman HA, Ruan Y, Blough MD, Nguyen SA, Kelly JJP, Cairncross JG, Weiss S. On target inhibition of JAK2/STAT3 signaling shows disease progression in orthotopic xenografts of molecularly heterogeneous human GBM-derived brain tumor stem cells. *Neuro Oncol*. 2012;E-publication ahead of print.
35. Luchman HA, Stechishin OD, Dang NH, Blough MD, Chesnelong C, Kelly JJ, Nguyen SA, Chan JA, Weljie AM, Cairncross JG, Weiss S. An in vivo patient-derived model of endogenous IDH1-mutant glioma. *Neuro Oncol*. 2012 Feb;14(2):184-191.
36. Stechishin OD, Luchman HA, Ruan Y, Blough MD, Nguyen SA, Kelly JJ, Cairncross JG, Weiss S. On-target JAK2/STAT3 inhibition slows disease progression in orthotopic xenografts of human glioblastoma brain tumor stem cells. *Neuro Oncol*. 2013 Feb;15(2):198-207.

37. Druker BJ. Current treatment approaches for chronic myelogenous leukemia. *Cancer J*. 2001 Jul-Aug;7 Suppl 1:S14-18.
38. Mauro MJ, Druker BJ. STI571: targeting BCR-ABL as therapy for CML. *Oncologist*. 2001;6(3):233-238.
39. O'Brien SG, Guilhot F, Larson RA, Gathmann I, Baccarani M, Cervantes F, Cornelissen JJ, Fischer T, Hochhaus A, Hughes T, Lechner K, Nielsen JL, Rousselot P, Reiffers J, Saglio G, Shepherd J, Simonsson B, Gratwohl A, Goldman JM, Kantarjian H, Taylor K, Verhoef G, Bolton AE, Capdeville R, Druker BJ. Imatinib compared with interferon and low-dose cytarabine for newly diagnosed chronic-phase chronic myeloid leukemia. *N Engl J Med*. 2003 Mar 13;348(11):994-1004.
40. Takano S YY, Kondo S, Suzuki H, Maruno T, Shirai S, Nose T. Concentration of vascular endothelial growth factor in the serum and tumor tissue of brain tumor patients. *Cancer Res*. 1996;56(9):2185-2190.
41. Johansson M, Brannstrom T, Bergenheim AT, Henriksson R. Spatial expression of VEGF-A in human glioma. *J Neurooncol*. 2002 Aug;59(1):1-6.
42. Vredenburgh JJ, Desjardins A, Herndon JE, 2nd, Dowell JM, Reardon DA, Quinn JA, Rich JN, Sathornsumetee S, Gururangan S, Wagner M, Bigner DD, Friedman AH, Friedman HS. Phase II trial of bevacizumab and irinotecan in recurrent malignant glioma. *Clin Cancer Res*. 2007 Feb 15;13(4):1253-1259.
43. Hurwitz H, Fehrenbacher L, Novotny W, Cartwright T, Hainsworth J, Heim W, Berlin J, Baron A, Griffing S, Holmgren E, Ferrara N, Fyfe G, Rogers B, Ross

- R, Kabbinavar F. Bevacizumab plus irinotecan, fluorouracil, and leucovorin for metastatic colorectal cancer. *N Engl J Med.* 2004 Jun 3;350(23):2335-2342.
44. Raizer JJ, Abrey LE, Lassman AB, Chang SM, Lamborn KR, Kuhn JG, Yung WK, Gilbert MR, Aldape KA, Wen PY, Fine HA, Mehta M, Deangelis LM, Lieberman F, Cloughesy TF, Robins HI, Dancey J, Prados MD, North American Brain Tumor C. A phase II trial of erlotinib in patients with recurrent malignant gliomas and nonprogressive glioblastoma multiforme postradiation therapy. *Neuro Oncol.* 2010 Jan;12(1):95-103.
45. Thiessen B, Stewart C, Tsao M, Kamel-Reid S, Schaiquevich P, Mason W, Easaw J, Belanger K, Forsyth P, McIntosh L, Eisenhauer E. A phase I/II trial of GW572016 (lapatinib) in recurrent glioblastoma multiforme: clinical outcomes, pharmacokinetics and molecular correlation. *Cancer Chemother Pharmacol.* 2010 Jan;65(2):353-361.
46. Uhm JH, Ballman KV, Wu W, Giannini C, Krauss JC, Buckner JC, James CD, Scheithauer BW, Behrens RJ, Flynn PJ, Schaefer PL, Dakhil SR, Jaeckle KA. Phase II evaluation of gefitinib in patients with newly diagnosed Grade 4 astrocytoma: Mayo/North Central Cancer Treatment Group Study N0074. *Int J Radiat Oncol Biol Phys.* 2011 Jun 1;80(2):347-353.
47. Sampson JH, Heimberger AB, Archer GE, Aldape KD, Friedman AH, Friedman HS, Gilbert MR, Herndon JE, 2nd, McLendon RE, Mitchell DA, Reardon DA, Sawaya R, Schmittling RJ, Shi W, Vredenburgh JJ, Bigner DD. Immunologic escape after prolonged progression-free survival with epidermal growth factor

- receptor variant III peptide vaccination in patients with newly diagnosed glioblastoma. *J Clin Oncol*. 2010 Nov 1;28(31):4722-4729.
48. Galanis E, Buckner JC, Maurer MJ, Kreisberg JI, Ballman K, Boni J, Peralba JM, Jenkins RB, Dakhil SR, Morton RF, Jaeckle KA, Scheithauer BW, Dancey J, Hidalgo M, Walsh DJ, North Central Cancer Treatment G. Phase II trial of temsirolimus (CCI-779) in recurrent glioblastoma multiforme: a North Central Cancer Treatment Group Study. *J Clin Oncol*. 2005 Aug 10;23(23):5294-5304.
49. Cloughesy TF, Yoshimoto K, Nghiemphu P, Brown K, Dang J, Zhu S, Hsueh T, Chen Y, Wang W, Youngkin D, Liao L, Martin N, Becker D, Bergsneider M, Lai A, Green R, Oglesby T, Koleto M, Trent J, Horvath S, Mischel PS, Mellinghoff IK, Sawyers CL. Antitumor activity of rapamycin in a Phase I trial for patients with recurrent PTEN-deficient glioblastoma. *PLoS Med*. 2008 Jan 22;5(1):e8.
50. Wen PY, Lee EQ, Reardon DA, Ligon KL, Alfred Yung WK. Current clinical development of PI3K pathway inhibitors in glioblastoma. *Neuro Oncol*. 2012 Jul;14(7):819-829.
51. Aaronson DS, Horvath CM. A road map for those who don't know JAK-STAT. *Science*. 2002 May 31;296(5573):1653-1655.
52. Heinrich PC, Behrmann I, Haan S, Hermanns HM, Muller-Newen G, Schaper F. Principles of interleukin (IL)-6-type cytokine signalling and its regulation. *Biochem J*. 2003 Aug 15;374(Pt 1):1-20.
53. Schindler C, Levy DE, Decker T. JAK-STAT signaling: from interferons to cytokines. *J Biol Chem*. 2007 Jul 13;282(28):20059-20063.

54. Huang S. Regulation of metastases by signal transducer and activator of transcription 3 signaling pathway: clinical implications. *Clin Cancer Res.* 2007 Mar 1;13(5):1362-1366.
55. Igaz P, Toth S, Falus A. Biological and clinical significance of the JAK-STAT pathway; lessons from knockout mice. *Inflamm Res.* 2001 Sep;50(9):435-441.
56. Yeh TC, Pellegrini S. The Janus kinase family of protein tyrosine kinases and their role in signaling. *Cell Mol Life Sci.* 1999 Sep;55(12):1523-1534.
57. O'Shea JJ, Gadina M, Schreiber RD. Cytokine signaling in 2002: new surprises in the Jak/Stat pathway. *Cell.* 2002 Apr;109 Suppl:S121-131.
58. Baxter EJ, Scott LM, Campbell PJ, East C, Fourouclas N, Swanton S, Vassiliou GS, Bench AJ, Boyd EM, Curtin N, Scott MA, Erber WN, Green AR. Acquired mutation of the tyrosine kinase JAK2 in human myeloproliferative disorders. *Lancet.* 2005 Mar 19-25;365(9464):1054-1061.
59. Briscoe J, Guschin D, Muller M. Signal transduction. Just another signalling pathway. *Curr Biol.* 1994 Nov 1;4(11):1033-1035.
60. Darnell JE, Jr., Kerr IM, Stark GR. Jak-STAT pathways and transcriptional activation in response to IFNs and other extracellular signaling proteins. *Science.* 1994 Jun 3;264(5164):1415-1421.
61. Bowman T, Garcia R, Turkson J, Jove R. STATs in oncogenesis. *Oncogene.* 2000 May 15;19(21):2474-2488.
62. Levy DE, Gilliland DG. Divergent roles of STAT1 and STAT5 in malignancy as revealed by gene disruptions in mice. *Oncogene.* 2000 May 15;19(21):2505-2510.

63. Bromberg J, Darnell JE, Jr. The role of STATs in transcriptional control and their impact on cellular function. *Oncogene*. 2000 May 15;19(21):2468-2473.
64. de la Iglesia N, Konopka G, Puram SV, Chan JA, Bachoo RM, You MJ, Levy DE, Depinho RA, Bonni A. Identification of a PTEN-regulated STAT3 brain tumor suppressor pathway. *Genes Dev*. 2008 Feb 15;22(4):449-462.
65. Lo HW, Cao XY, Zhu H, Ali-Osman F. Cyclooxygenase-2 Is a Novel Transcriptional Target of the Nuclear EGFR-STAT3 and EGFRvIII-STAT3 Signaling Axes. *Molecular Cancer Research*. 2010 Feb;8(2):232-245.
66. Guryanova OA, Wu Q, Cheng L, Lathia JD, Huang Z, Yang J, MacSwords J, Eyler CE, McLendon RE, Heddleston JM, Shou W, Hambardzumyan D, Lee J, Hjelmeland AB, Sloan AE, Bredel M, Stark GR, Rich JN, Bao S. Nonreceptor tyrosine kinase BMX maintains self-renewal and tumorigenic potential of glioblastoma stem cells by activating STAT3. *Cancer Cell*. 2011 Apr 12;19(4):498-511.
67. Peñuelas S, Anido J, Prieto-Sánchez RM, Folch G, Barba I, Cuartas I, García-Dorado D, Poca MA, Sahuquillo J, Baselga J, Seoane J. TGF-beta increases glioma-initiating cell self-renewal through the induction of LIF in human glioblastoma. *Cancer Cell*. 2009;15(4):315-327.
68. Wang H, Lathia JD, Wu Q, Wang J, Li Z, Heddleston JM, Eyler CE, Elderbroom J, Gallagher J, Schuschu J, MacSwords J, Cao Y, McLendon RE, Wang XF, Hjelmeland AB, Rich JN. Targeting interleukin 6 signaling suppresses glioma stem cell survival and tumor growth. *Stem Cells*. 2009 Oct;27(10):2393-2404.



69. Cao Y, Lathia JD, Eyster CE, Wu Q, Li Z, Wang H, McLendon RE, Hjelmeland AB, Rich JN. Erythropoietin Receptor Signaling Through STAT3 Is Required For Glioma Stem Cell Maintenance. *Genes Cancer*. 2010;1(1):50-61.
70. Brantley EC, Nabors LB, Gillespie GY, Choi YH, Palmer CA, Harrison K, Roarty K, Benveniste EN. Loss of protein inhibitors of activated STAT-3 expression in glioblastoma multiforme tumors: implications for STAT-3 activation and gene expression. *Clin Cancer Res*. 2008 Aug 1;14(15):4694-4704.
71. Lindemann C, Hackmann O, Delic S, Schmidt N, Reifenberger G, Riemenschneider MJ. SOCS3 promoter methylation is mutually exclusive to EGFR amplification in gliomas and promotes glioma cell invasion through STAT3 and FAK activation. *Acta Neuropathologica*. 2011 Aug;122(2):241-251.
72. Yu H, Pardoll D, Jove R. STATs in cancer inflammation and immunity: a leading role for STAT3. *Nat Rev Cancer*. 2009 Nov;9(11):798-809.
73. Dasgupta A, Raychaudhuri B, Haqqi T, Prayson R, Van Meir EG, Vogelbaum M, Haque SJ. Stat3 activation is required for the growth of U87 cell-derived tumours in mice. *Eur J Cancer*. 2009 Mar;45(4):677-684.
74. Gu J, Li G, Sun T, Su Y, Zhang X, Shen J, Tian Z, Zhang J. Blockage of the STAT3 signaling pathway with a decoy oligonucleotide suppresses growth of human malignant glioma cells. *J Neurooncol*. 2008 Aug;89(1):9-17.
75. Shen J, Li R, Li G. Inhibitory effects of decoy-ODN targeting activated STAT3 on human glioma growth in vivo. *In Vivo*. 2009 Mar-Apr;23(2):237-243.

76. Li GH, Wei H, Lv SQ, Ji H, Wang DL. Knockdown of STAT3 expression by RNAi suppresses growth and induces apoptosis and differentiation in glioblastoma stem cells. *Int J Oncol*. 2010 Jul;37(1):103-110.
77. Villalva C, Martin-Lannere S, Cortes U, Dkhissi F, Wager M, Le Corf A, Tourani JM, Dusanter-Fourt I, Turhan AG, Karayan-Tapon L. STAT3 is essential for the maintenance of neurosphere-initiating tumor cells in patients with glioblastomas: a potential for targeted therapy? *Int J Cancer*. 2011 Feb 15;128(4):826-838.
78. Borghouts C, Kunz C, Delis N, Groner B. Monomeric recombinant peptide aptamers are required for efficient intracellular uptake and target inhibition. *Molecular Cancer Research*. 2008 Feb;6(2):267-281.
79. Fuh B, Sobo M, Cen L, Josiah D, Hutzen B, Cisek K, Bhasin D, Regan N, Lin L, Chan C, Caldas H, DeAngelis S, Li C, Li PK, Lin J. LLL-3 inhibits STAT3 activity, suppresses glioblastoma cell growth and prolongs survival in a mouse glioblastoma model. *Br J Cancer*. 2009 Jan 13;100(1):106-112.
80. Lin L, Hutzen B, Li PK, Ball S, Zuo M, DeAngelis S, Foust E, Sobo M, Friedman L, Bhasin D, Cen L, Li C, Lin J. A novel small molecule, LLL12, inhibits STAT3 phosphorylation and activities and exhibits potent growth-suppressive activity in human cancer cells. *Neoplasia*. 2010 Jan;12(1):39-50.
81. Rahaman SO, Harbor PC, Chernova O, Barnett GH, Vogelbaum MA, Haque SJ. Inhibition of constitutively active Stat3 suppresses proliferation and induces apoptosis in glioblastoma multiforme cells. *Oncogene*. 2002 Dec 5;21(55):8404-8413.

82. Iwamaru A, Szymanski S, Iwado E, Aoki H, Yokoyama T, Fokt I, Hess K, Conrad C, Madden T, Sawaya R, Kondo S, Priebe W, Kondo Y. A novel inhibitor of the STAT3 pathway induces apoptosis in malignant glioma cells both in vitro and in vivo. *Oncogene*. 2007 Apr 12;26(17):2435-2444.
83. Lo HW, Cao X, Zhu H, Ali-Osman F. Constitutively activated STAT3 frequently coexpresses with epidermal growth factor receptor in high-grade gliomas and targeting STAT3 sensitizes them to Iressa and alkylators. *Clin Cancer Res*. 2008 Oct 1;14(19):6042-6054.
84. Weissenberger J, Priester M, Bernreuther C, Rakel S, Glatzel M, Seifert V, Kogel D. Dietary curcumin attenuates glioma growth in a syngeneic mouse model by inhibition of the JAK1,2/STAT3 signaling pathway. *Clin Cancer Res*. 2010 Dec 1;16(23):5781-5795.
85. McFarland BC, Ma JY, Langford CP, Gillespie GY, Yu H, Zheng Y, Nozell SE, Huszar D, Benveniste EN. Therapeutic potential of AZD1480 for the treatment of human glioblastoma. *Mol Cancer Ther*. 2011 Dec;10(12):2384-2393.
86. Sai K, Wang S, Balasubramanian V, Conrad C, Lang FF, Aldape K, Szymanski S, Fokt I, Dasgupta A, Madden T, Guan S, Chen Z, Alfred Yung WK, Priebe W, Colman H. Induction of cell-cycle arrest and apoptosis in glioblastoma stem-like cells by WP1193, a novel small molecule inhibitor of the JAK2/STAT3 pathway. *J Neurooncol*. 2012 May;107(3):487-501.
87. Hussain SF, Kong LY, Jordan J, Conrad C, Madden T, Fokt I, Priebe W, Heimberger AB. A novel small molecule inhibitor of signal transducers and activators of

- transcription 3 reverses immune tolerance in malignant glioma patients. *Cancer Res.* 2007 Oct 15;67(20):9630-9636.
88. Tefferi A. JAK inhibitors for myeloproliferative neoplasms: clarifying facts from myths. *Blood.* 2012 Mar 22;119(12):2721-2730.
89. Thoma G, Nuninger F, Falchetto R, Hermes E, Tavares GA, Vangrevelinghe E, Zerwes HG. Identification of a potent Janus kinase 3 inhibitor with high selectivity within the Janus kinase family. *J Med Chem.* 2011 Jan 13;54(1):284-288.
90. Burmester GR, Blanco R, Charles-Schoeman C, Wollenhaupt J, Zerbini C, Benda B, Gruben D, Wallenstein G, Krishnaswami S, Zwillich SH, Koncz T, Soma K, Bradley J, Mebus C. Tofacitinib (CP-690,550) in combination with methotrexate in patients with active rheumatoid arthritis with an inadequate response to tumour necrosis factor inhibitors: a randomised phase 3 trial. *Lancet.* 2013 Feb 9;381(9865):451-460.
91. van der Heijde D, Tanaka Y, Fleischmann R, Keystone E, Kremer J, Zerbini C, Cardiel MH, Cohen S, Nash P, Song YW, Tegzova D, Wyman BT, Gruben D, Benda B, Wallenstein G, Krishnaswami S, Zwillich SH, Bradley JD, Connell CA. Tofacitinib (CP-690,550) in patients with rheumatoid arthritis receiving methotrexate: twelve-month data from a twenty-four-month phase III randomized radiographic study. *Arthritis Rheum.* 2013 Mar;65(3):559-570.
92. Mamolo C, Harness J, Tan H, Menter A. Tofacitinib (CP-690,550), an oral Janus kinase inhibitor, improves patient-reported outcomes in a phase 2b, randomized,

- double-blind, placebo-controlled study in patients with moderate-to-severe psoriasis. *J Eur Acad Dermatol Venereol*. 2013 Jan 7.
93. Ports WC, Khan S, Lan S, Lamba M, Bolduc C, Bissonnette R, Papp K. A randomised Phase 2a efficacy and safety trial of the topical Janus kinase inhibitor tofacitinib in the treatment of chronic plaque psoriasis. *Br J Dermatol*. 2013 Feb 6.
94. Liew SH, Nichols KK, Klamerus KJ, Li JZ, Zhang M, Foulks GN. Tofacitinib (CP-690,550), a Janus kinase inhibitor for dry eye disease: results from a phase 1/2 trial. *Ophthalmology*. 2012 Jul;119(7):1328-1335.
95. Sandborn WJ, Ghosh S, Panes J, Vranic I, Su C, Rousell S, Niezychowski W. Tofacitinib, an oral Janus kinase inhibitor, in active ulcerative colitis. *N Engl J Med*. 2012 Aug 16;367(7):616-624.
96. Vincenti F, Tedesco Silva H, Busque S, O'Connell P, Friedewald J, Cibrik D, Budde K, Yoshida A, Cohn S, Weimar W, Kim YS, Lawendy N, Lan SP, Kudlacz E, Krishnaswami S, Chan G. Randomized phase 2b trial of tofacitinib (CP-690,550) in de novo kidney transplant patients: efficacy, renal function and safety at 1 year. *Am J Transplant*. 2012 Sep;12(9):2446-2456.
97. Ju W, Zhang M, Jiang JK, Thomas CJ, Oh U, Bryant BR, Chen J, Sato N, Tagaya Y, Morris JC, Janik JE, Jacobson S, Waldmann TA. CP-690,550, a therapeutic agent, inhibits cytokine-mediated Jak3 activation and proliferation of T cells from patients with ATL and HAM/TSP. *Blood*. 2011 Feb 10;117(6):1938-1946.
98. Deuse T, Velotta JB, Hoyt G, Govaert JA, Taylor V, Masuda E, Herlaar E, Park G, Carroll D, Pelletier MP, Robbins RC, Schrepfer S. Novel immunosuppression:

- R348, a JAK3- and Syk-inhibitor attenuates acute cardiac allograft rejection. *Transplantation*. 2008 Mar 27;85(6):885-892.
99. Chang BY, Zhao F, He X, Ren H, Braselmann S, Taylor V, Wicks J, Payan DG, Grossbard EB, Pine PR, Bullard DC. JAK3 inhibition significantly attenuates psoriasiform skin inflammation in CD18 mutant PL/J mice. *J Immunol*. 2009 Aug 1;183(3):2183-2192.
100. Chojnacki A, Kelly JJ, Hader W, Weiss S. Distinctions between fetal and adult human platelet-derived growth factor-responsive neural precursors. *Ann Neurol*. 2008 Aug;64(2):127-142.
101. Ostermann S, Csajka C, Buclin T, Leyvraz S, Lejeune F, Decosterd LA, Stupp R. Plasma and cerebrospinal fluid population pharmacokinetics of temozolomide in malignant glioma patients. *Clin Cancer Res*. 2004 Jun 1;10(11):3728-3736.
102. Velotta JB, Deuse T, Haddad M, Masuda E, Park G, Carroll D, Taylor V, Robbins RC, Schrepfer S. A novel JAK3 inhibitor, R348, attenuates chronic airway allograft rejection. *Transplantation*. 2009 Mar 15;87(5):653-659.
103. Verstovsek S. Therapeutic potential of Janus-activated kinase-2 inhibitors for the management of myelofibrosis. *Clin Cancer Res*. 2010 Apr 1;16(7):1988-1996.
104. Weaver JL. Establishing the carcinogenic risk of immunomodulatory drugs. *Toxicol Pathol*. 2012;40(2):267-271.
105. Fishman JA. Infections in immunocompromised hosts and organ transplant recipients: essentials. *Liver Transpl*. 2011 Nov;17 Suppl 3:S34-37.